Energy Balance Climate Models

GERALD R. NORTH[1]

Laboratory for Atmospheric Sciences, NASA Goddard Space Flight Center, Greenbelt, Maryland 20771

ROBERT F. CAHALAN[2] AND JAMES A. COAKLEY, JR.

National Center for Atmospheric Research, Boulder, Colorado 80307

An introductory survey of the global energy balance climate models is presented with an emphasis on analytical results. A sequence of increasingly complicated models involving ice cap and radiative feedback processes are solved, and the solutions and parameter sensitivities are studied. The model parameterizations are examined critically in light of many current uncertainties. A simple seasonal model is used to study the effects of changes in orbital elements on the temperature field. A linear stability theorem and a complete nonlinear stability analysis for the models are developed. Analytical solutions are also obtained for the linearized models driven by stochastic forcing elements. In this context the relation between natural fluctuation statistics and climate sensitivity is stressed.

CONTENTS

1. INTRODUCTION

The theory of climate has received much attention in the last few years. The evolution of high-speed computers and the development of numerical weather prediction models have made the simulation of climate at least ponderable. The global scale collection and analysis of observations have provided a base for developing and verifying models. In addition, the extraction of paleoclimatic information from various sources is beginning to produce a legible record of climatic history. Preliminary studies of the earth's climate suggest that the present state may be a delicate one possibly vulnerable to unintentional adverse changes by man's activities. As it demands more and more from the earth's dwindling resources,

the growing human population becomes less able to cope with climatic change. As a result the forecasting of future climates becomes increasingly important. Evidently, the time has come to develop mathematical models of the climate.

The purpose of this review is to present an introductory survey of simple climate models based upon elementary heat balance considerations. The paper is intended to be pedagogical, introducing complicated subjects by way of solvable examples. The review begins with the fundamental principles that govern planetary climates and proceeds to develop a theory for one-dimensional climate models.

Schneider and Dickinson [1974] have surveyed many approaches to climate modeling. Foremost in their discussion is the hierarchy of climate models. A wide range of models may be constructed, based upon the choice and number of degrees of freedom to be included. General circulation models (GCM's) can have up to a million degrees of freedom, while the simplest models have only a few. Although, in principle, GCM's could become physically realistic, they are expensive and cumbersome. The artificial climates generated by these models are typically as complicated and inscrutable as the earth's climate. Their major advantage (once perfected) will be their controllability, that is, the possibility of testing hypotheses by changing boundary conditions, a luxury not afforded by the real climate.

Because of the expense and complicated output of large GCM's a variety of simplified initial value models are presently under construction for use in sensitivity experiments [e.g., *Held and Suarez*, 1978; *Gates and Schlesinger*, 1977]. It is hoped that these models will produce climates and climate change responses similar to those of their larger counterparts.

Since the climate is represented by the long-term averages of atmospheric variables, one promising approach is to construct equations in terms of these averaged quantities. Recently, there have been many attempts to construct and study such equations. The resulting models are referred to as 'statistical dynamical models' (SDM's) and were reviewed by *Saltzman* [1978].

Among the SDM's are the few variable models. If only the vertical dimension is retained, one obtains the radiative-convective models reviewed by *Ramanathan and Coakley* [1978]. The advantage of these models is that they can be used to

compute radiative transfer in detail and therefore any climatic feedback mechanisms associated with radiation may be carefully studied.

If we characterize a column of the earth-atmosphere system by a single number, say, the sea level temperature, we develop models with only horizontal dimensions. Zonal averaging of such models leads us to the one-dimensional climate models. Models of this type have been studied for some years [Ångström, 1928; Fritz, 1960; Öpik, 1965; Eriksson, 1968]. Renewed interest in these models was stimulated by Budyko [1968, 1969, 1972] and Sellers [1969]. These two investigators independently derived one-dimensional models based upon the thermodynamic equation. Each term in the equation was written in terms of the sea level temperature field. In doing so they distilled the climate problem into a one-dimensional, steady state, boundary value problem that was solved for the temperature field. Although the equations were nonlinear, solutions could be extracted by either analytical or reliable numerical procedures. One was then in a position to vary such 'given' parameters as the solar constant to study the model response.

Budyko and Sellers arrived at the surface temperature dependence of the individual terms in the energy balance equations through independent studies of the observed heat fluxes. Not surprisingly, the functional forms were rather different from each other. Nevertheless, both models yielded the present climate as solutions. Furthermore, both predicted the same high sensitivity to changes in the solar constant. They predicted that if the solar constant were lowered by only a few percent, the polar ice caps would expand catastrophically until the globe became completely covered by ice. The Budyko-Sellers models form the basis for this review.

A number of questions immediately arise from the pioneering studies just mentioned. For instance, to what extent are the models equivalent to each other, and, for that matter, do they behave like more sophisticated models possibly imitating the earth's climate? To what extent is the extreme climate sensitivity of these models dependent upon the parameterizations used to relate the surface temperature to the heat fluxes? What is the nature of the model climate solutions; for instance, is the model solution unique; is it stable to small perturbations? Are the models consistent with the history of the solar system? What is the range of space and time scales for which the models are valid? Can the models suggest new measurements or data reduction methods that would further the development of a climate theory? Are there any ways to test the validity of the models; for instance, would they apply to the other planets? Can the models be extended to include seasonal and regional effects? Can the models test various theories of the ice ages? Finally, can the models be used to define research problems for the more comprehensive models? Some of these questions have been answered in the last few years, while others remain open.

One appealing feature of the Budyko-Sellers models is their simplicity. This simplicity facilitates the use of the models as teaching tools. It therefore seems appropriate in this review to use elementary analytical methods whenever possible. In this way we can keep the physical mechanisms before us at all times. As a result the inevitable fudge factors will be explicit. More emphasis will be placed upon theoretical rather than numerical results because the latter are subject to change with new observations and new developments in parameterization theory. Although the theory of energy balance models has had many contributors with varied approaches, we have attempted to develop the theory whenever possible in a simple, uniform manner, often drawing upon the work of others.

The review is divided into nine sections. After reading section 2 most of the other sections can be read independently of each other.

2. INTRODUCTION TO HEAT BALANCE MODELS

To begin, we introduce the concept of global radiative heat balance. For simplicity we assume that the earth emits radiation as a blackbody. In radiative equilibrium the rate at which solar radiation is absorbed matches the rate at which infrared radiation is emitted. The condition of radiative equilibrium is given by

$$4\pi R^2 \sigma T_R^4 = \sigma_0(1 - \alpha_p)\pi R^2 \tag{1}$$

where T_R is the effective radiating temperature of the planet; R is the radius of the planet; σ_0 is the solar constant, taken in this section to be 1340 W m^{-2}; σ is the Stefan-Boltzmann constant, 0.56687×10^{-7} W m^{-2} K^{-4}; and α_p is the planetary albedo defined as

$$\alpha_p = \frac{1}{2}\int_{-1}^{1} dx\, S(x)\alpha(x) \tag{2}$$

where x is the sine of latitude; $\alpha(x)$ is the albedo at latitude x; and $S(x)$ is the mean annual distribution of radiation reaching the top of the atmosphere, normalized so that the integral of $S(x)$ from 0 to 1 is unity. $S(x)$ and its seasonal analog $S(x, t)$ may be computed exactly [Sellers, 1965], but for this discussion we may use the approximate form [North, 1975a; North and Coakley, 1979]

$$S(x) \cong 1 + S_2 P_2(x) \tag{3}$$

with $S_2 = -0.477$ and $P_2(x)$ the second Legendre polynomial, $P_2(x) = \frac{1}{2}(3x^2 - 1)$. With this approximation, $S(x)$ is a parabola in x, having zero derivative at the equator ($x = 0$) and falling to a value of 0.523 at the pole ($x = 1$). We note in passing that x is a convenient variable to use in zonal average applications because dx is proportional to the area of a latitude strip and therefore the area average of $q(x)$ for the region spanned by Δx is given by

$$\bar{q} = \int_{\Delta x} q(x)\, dx/\Delta x \tag{4}$$

Using a value of 0.30 for α_p [Ellis et al., 1978], we compute $T_R = 254.6$ K for the earth's radiative temperature. Clearly, this is much colder than the observed sea level average temperature, which (for the whole globe) is 287.4 K. The major part of this difference is, of course, due to the so-called greenhouse effect of the atmosphere, to be discussed later.

Let us now compute the fundamental sensitivity parameter β_0, defined by

$$\beta_0 = \frac{\sigma_0}{100} \frac{dT_0}{d\sigma_0} \tag{5}$$

where the subscript 0 on T refers to the global average value. The parameter β_0 is a measure of the change in global average temperature due to a 1% change in the solar constant. For all climate models, β_0 is the first quantity to compute because the sensitivity of the model to any perturbation is roughly proportional to β_0 (cf. sections 7 and 8).

With α_p constant the simple model defined by (1) gives

$$\beta_0(\text{black radiator}) = T_R/400 = 0.63 \text{ K} \tag{6}$$

This number represents the sensitivity of a system with no feedbacks, and it is a standard for comparison with all climate models.

The sensitivity of the actual climate is influenced by a myriad of feedback processes [Schneider and Dickinson, 1974]. For example, changes in planetary temperature might change the emissivity or reflectivity and thereby modify the sensitivity. Many of these agents and linkages have yet to be identified. Many of the details of the known and suspected feedbacks remain a mystery. Some of these uncertainties are discussed in section 4. Here we introduce some simple models to illustrate the potential impact of known feedbacks on climate.

It is well to note that the value taken here for the solar constant σ_0 (1340 W m^{-2}) is different from that used in section 4 (1360 W m^{-2}) so that we do not have to repeat published calculations. In fact, various modelers have used different values for this parameter in their sensitivity studies. Generally, the sensitivity results are not sensitive to the present value of the solar constant. Errors introduced in this way tend to be partially compensated for in adjusting other unknown parameters to force the model's unperturbed climate to fit the present climate, a process sometimes referred to as 'tuning.' Incidentally, the exact value of the solar constant and its constancy in time are the subject of considerable experimental activity in both rocket measurements [Willson et al., 1980] and satellite measurements [Hickey et al., 1980]. The best current value from the Nimbus 7 satellite is 1376 W m^{-2}.

Global Models With Feedback

Feedbacks affect the sensitivity through their influence on the radiative fluxes absorbed and emitted. Often the net effect of the feedbacks is inferred from empirical data. We begin with the flux of infrared radiation emitted by the earth.

Budyko [1969] suggested that the infrared radiation to space can be represented as a linear function of the surface temperature T (in degrees Celsius):

$$I = A + BT \qquad (7)$$

where A and B are constants deduced from observations. On the basis of data from the northern hemisphere [North and Coakley, 1979] we find that $A = 203.3$ W m^{-2} and $B = 2.09$ W m^{-2} °C^{-1} gives the best fit between the fluxes calculated using (7) and those observed. The energy balance may be written as

$$A + BT_0 = Q(1 - \alpha_p) \qquad (8)$$

where Q is $\sigma_0/4$. Using $(1 - \alpha_p) = 0.70$, we arrive at $T_0 = 14.97$°C, which agrees with the northern hemisphere value (14.9°C). The coefficients A and B take into account average cloudiness conditions, the effects of infrared absorbing gases, and the variability of water vapor. For comparison a linear expansion of $\sigma(273 + T)^4$ would lead to 'black radiator' coefficients $A_b = 314.9$ W m^{-2} and $B_b = 4.61$ W m^{-2} °C^{-1}.

For constant albedo the sensitivity of this 'greenhouse model' is

$$\beta_0(\text{greenhouse}) = (A + BT_0)/100B = 1.12°C \qquad (9)$$

We deduce that the presence of an atmosphere increases the sensitivity of the climate. This effect is referred to as a 'positive feedback,' since it increases the sensitivity over that of a blackbody radiator.

Let us examine the reasons for this positive feedback. Con-

sider a planet surrounded by a shield at temperature T_1. We will assume that this 'atmosphere' does not absorb solar radiation but perfectly absorbs infrared radiation. We imagine the shield to be in equilibrium so that it radiates (net up and down) at a rate equal to the rate at which it absorbs. As a result, T_1 is related to T_0 by

$$\sigma T_0^4 = 2\sigma T_1^4 \qquad (10)$$

Similarly, if the surface is in radiative equilibrium, then T_0 is given by

$$\sigma T_0^4 = \sigma T_1^4 + Q(1 - \alpha_p) \qquad (11)$$

From (10) we deduce that T_0 is greater than T_1 by a factor of $2^{1/4}$ (≈ 1.19). Furthermore, by combining (10) and (11) we see that T_1 is the effective radiating temperature of the planet. For $T_1 = 254$ K we compute $T_0 = 302$ K. Thus a single black shield approximates the greenhouse correction of the earth's atmosphere. Combining (10) and (11) and differentiating with respect to Q, keeping the albedo constant, we obtain

$$\beta_0(\text{black shield}) = T_0/400 = 0.76 \text{ K} \qquad (12)$$

Although the black shield approximates the atmosphere's greenhouse effect, it fails to account for the increased sensitivity when the atmosphere is present.

The most probable reason for the enhancement is the variable concentration of water vapor. Water vapor is a significant absorber in the infrared. On the average the amount of water vapor in the atmosphere increases as the temperature increases [Manabe and Wetherald, 1967]. To allow for this increase, we should allow the number of black shields to increase with temperature. The empirical coefficients in Budyko's formula presumably take this effect into account. There are, of course, other feedbacks that affect emission, and their influence is also reflected in the coefficients. In the next section we shall return to the Budyko formula and discuss its validity.

Let us now examine the ice cap albedo feedback. If the earth had no ice or snow but it had 50% cloudiness, the local co-albedo (1 − albedo) would be approximately $a_f(x) = 0.70$; similarly, an ice-covered planet would have co-albedo $a_i(x) = 0.38$. Using (8), we compute $T_0 = 15.0$°C for the ice-free planet and $T_0 = -36.4$°C for the ice-covered planet. Of course, the earth lies between these extremes.

Let us propose a crude model for the ice cap size. Suppose that the edge of the ice cap is denoted by $x = x_s$. Then suppose $x_s = 1$ for $T_0 > 15°$, $x_s = 0$ for $T_0 < -15°$, and in between, $x_s = 1 + (T_0 - 15)/30$. We may then use a_f for $0 < x < x_s$ and a_i for $x_s < x < 1$. From (3) the planetary co-albedo would then be given by

$$\bar{a} = 1 - \alpha_p$$
$$= a_i + (a_f - a_i)[x_s + \tfrac{1}{2} S_2(x_s - x_s^3)] = H_0[x_s(T_0)] \qquad (13)$$

The notation H_0 for the planetary co-albedo will prove useful later. $H_0[x_s(T_0)]$ is represented by the solid curve in Figure 1. To find solutions for (8), we plot the outgoing IR divided by Q, represented by the dashed curve in Figure 1. For the present solar constant we obtain three roots. The root labeled I corresponds to the present climate, root II to an intermediate climate with the planet having about 30% of its area covered by ice, and root III to an ice-covered planet. Such multiple solutions of zero-dimensional models were noted by Sellers [1974], Crafoord and Källén [1978], and Fraedrich [1978].
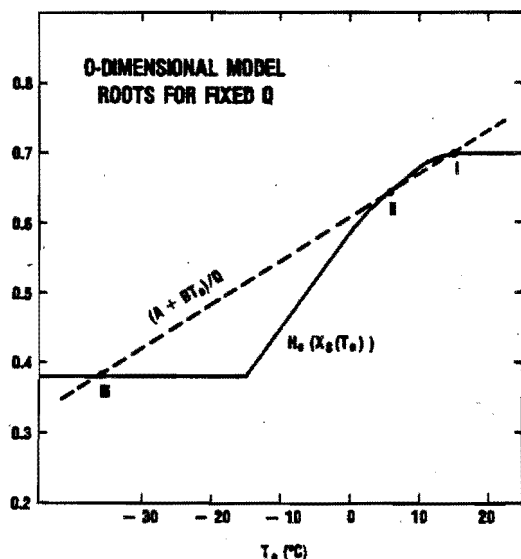
Fig. 1. Fraction of solar radiation absorbed (solid curve), $H_0[x_s(T_0)]$ (equation (13)), for the zero-dimensional global climate model with variable ice cap. The dashed curve shows the outgoing infrared energy per unit area per unit time divided by the present solar constant (divided by 4). Intersections of these curves are roots corresponding to steady state climates: root I corresponds to the present climate, root II to a large ice cap solution, and root III to a totally ice-covered planet.

In Figure 1 we have a qualitative picture of the model climates. If Q is decreased, the dashed curve is scaled upward, and roots II and III merge together and then disappear, leaving only the deep freeze, root III. If the solar constant is increased, roots II and III coalesce, and we are left only with an ice-free earth, Root I. Figure 2 shows T_0 as a function of Q.

The example just given illustrates the rich structure of even the simplest ice feedback model. The multiple branch structure shown in Figure 2 persists in models with latitude dependence and even exists in GCM's [*Wetherald and Manabe,* 1975].

One-Dimensional Models and Transport

After the zero-dimensional models, the next models to be studied include latitude dependence. This additional degree of freedom forces us to consider the horizontal transport of heat by the geophysical fluid system. In the treatment of this transport we will have to make drastic idealizations to keep the mathematics manageable.

In the latitude-dependent models we assume that the rate at which heat enters each infinitesimal latitude belt during the year is exactly balanced by the loss rate. The individual terms considered are schematically represented for the ith strip by

(net horizontal transport out)$_i$ +. (infrared out)$_i$
$$= \text{(solar absorbed)}_i \qquad (14)$$

A common factor, the area of the strip, may be canceled throughout, so that the remaining terms have units of energy per unit area per unit time (watts per square meter).

We proceed with the crucial simplifying assumption that each term in (14) may be represented as a function of the zonally averaged sea level (1000 mbar) temperature field $T(x_i)$. Once the parameterization formulae for the individual terms in (14) are found, we solve the system of equations represented by (14) for all indices i simultaneously. It is usually necessary to impose a boundary condition at the poles, since

mathematical systems like (14) often have an unphysical solution (irregular solution) that diverges at the poles. By imposing the condition that the flux of horizontal heat into the pole vanishes, we systematically eliminate such spurious model climates.

To see how the model behaves, let us examine a few extreme cases. We adopt the Budyko formula (7) for infrared radiation at each latitude, and we adopt an ice cap parameterization that is also due to *Budyko* [1969], namely, that the ice cap edge extends to the mean annual isotherm

$$T(x_s) = T_s = -10°C \qquad (15)$$

For simplicity we take the co-albedo $a(x, x_s)$ to be discontinuous at the ice cap edge. Note that x_s must come somehow from (15) rather than from the linear relation with T_0 that was adopted in the global average model.

For the case that the horizontal transport is infinite, the planetary surface must be isothermal. This model is similar to the global average model except that the span between $-15°$ and $15°C$ shown in Figure 1 is compressed to a vertical line centered at $-10°C$. The solution branches are easily shown to be given by the dashed lines in Figure 2. The physical interpretation is obtained by following a quasi-static change in Q down branch I of the solution. When the dark (isothermal) planet's temperature reaches $-10°C$, the planet suddenly turns white, and its new equilibrium temperature must be about $-44°C$.

For the case with no transport the energy balance equation becomes

$$A + BT(x) = QS(x)a(x, x_s) \qquad (16)$$

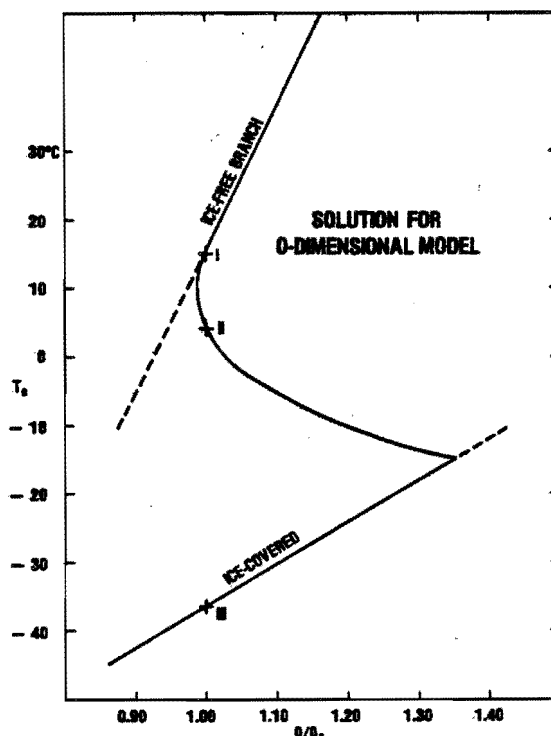Fig. 2. Steady-state temperatures corresponding to the climate solutions for the zero-dimensional climate model with variable ice cap as a function of solar constant in units of its present value (solid curve). The roots I, II, and III correspond to those in Figure 1. The dashed curves show the solutions that would be obtained in the case of infinite horizontal heat transport in which the planet is isothermal.

at each latitude. We assume further that at $x = x_s$ the co-albedo $a(x, x_s)$ becomes the average of a_i and a_f.

Applying (16) at $x = x_s$ and using (15), we obtain

$$Q(x_s) = (A + BT_s)/S(x_s)\hat{a} \qquad (17)$$

with $\hat{a} = (a_i + a_f)/2$. Expression (17) gives the solar constant Q needed to maintain the ice line at a particular latitude given by x_s. The curved line in Figure 3 is computed by using (17). The lower flat line $(x_s = 0)$ is obtained by starting with complete ice cover $(Q/Q_0 \ll 0.8)$ and raising the solar constant quasi-statically until the equatorial temperature reaches $-10°C$, which occurs at $Q/Q_0 = 1.17$). Similarly, the upper flat portion is obtained by lowering the solar constant from $Q/Q_0 \gg 2.0$ on the ice-free planet until the pole reaches $-10°C$. The peculiar solution lines emanating from the curve in Figure 3 are called 'twigs' by mathematicians. We shall return to the structure of these solutions later.

The models discussed thus far present a paradox. If the sun's luminosity has risen from a value of 20–40% lower than its current level, as virtually all solar evolution theories indicate [Newman and Rood, 1977], then why is the earth not covered with ice? The models indicate that if the solar constant is raised quasi-statically from, say, three quarters of its present value up to its present value, the model stays on the lower branch of the solution curve whether the transport is infinite or zero. Furthermore, we shall see that this result holds in every model studied in this paper. We are not in a position to resolve this solar evolution–climate model contradiction, but conjectures have been ventured: not enough moisture is available at the right places to generate total ice cover; other negative feedbacks are present, perhaps related to cloudiness change (our calculations are based on present cloud cover); and the composition of the atmosphere was different in the past such that a larger greenhouse effect prevented the ice cover [Sagan and Mullen, 1972; Owen et al., 1979; Hart, 1978; Budyko, 1977].

Clearly, the no-transport model bears little resemblance to the earth, since a solar constant 70% greater than the present value is required to push the ice cap back to $x_s = 0.95$ (its present location). With a Q of 1.7 times its present value and $x_s = 0.95$ the planetary average temperature becomes $T_0 = 93°C$. Aside from the unrealistic values obtained for T_0 and x_s, (16) suggests that $T(x)$ has a discontinuity of the order of $50°C$ at $x = x_s$. Transport, of course, tends to smooth this discontinuity.
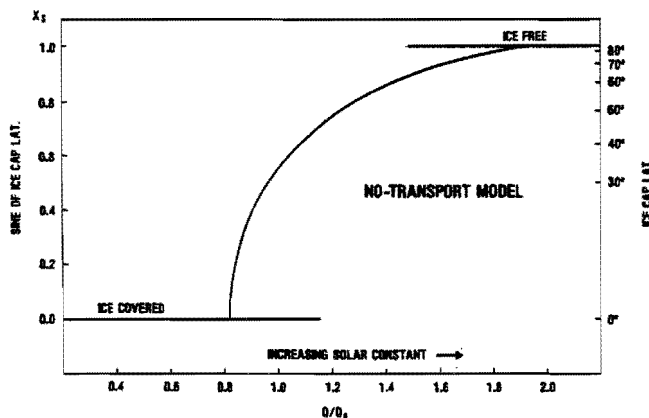
Fig. 3. Sine of steady state ice cap edge latitude x_s versus solar constant in units of its present value for a one-dimensional climate model with no horizontal heat transports (cf. equation (17)).
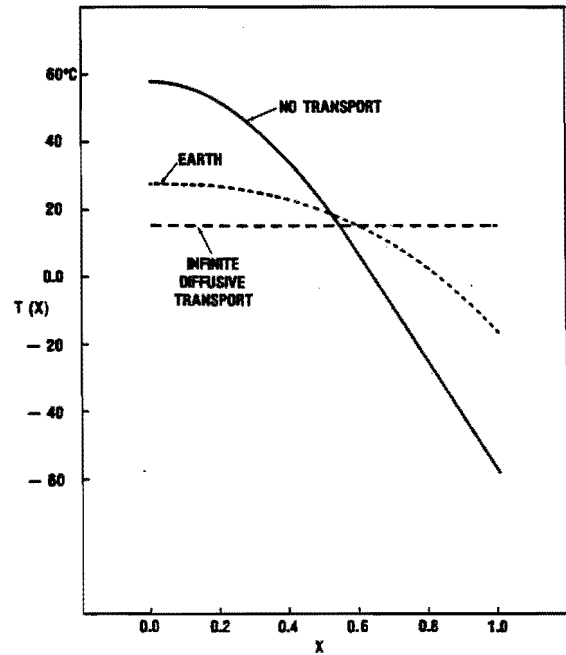
Fig. 4. Temperature (degrees Celsius) versus sine of latitude for the cases of no transport, infinite transport, and earth (schematic).

Before proceeding with a finite transport model, let us look at the zonal average temperatures obtained for the extreme cases of infinite and zero transport. For the absorption we take observed (northern hemisphere) mean annual values which are reasonably well represented by

$$a(x) = a_0 + a_2 P_2(x) \qquad (18)$$

with $a_0 = 0.681$ and $a_2 = -0.202$ [North and Coakley, 1979]. The planetary average temperature is obtained by integrating (16) over x:

$$A + BT_0 = Q \int_0^1 dx \, S(x)a(x) \qquad (19)$$

Using the constants specified earlier, we obtain $T_0 = 14.97°C$. Figure 4 shows $T(x)$ (solid curve) for the no-transport, no-ice-feedback case computed directly from (16). For comparison the figure also shows the infinite transport case (dashed line), which yields an isothermal $14.97°C$ planet, and the temperature observed for the earth. The transport has the obvious effect of warming the pole and cooling the equator. It maintains, however, the roughly parabolic shape of the no-transport case.

Consider the addition of a transport term to the heat balance equation. The geophysical fluids transport heat through their mean and transitory (eddy) motions. If we were to average the atmospheric velocity field through, say, a month and around a latitude circle, we would sample many statistically uncorrelated eddy processes. A first model for the atmosphere is a geophysical fluid having a random velocity field. We might take the heat content as a passive scalar being carried by the fluid. Equal amounts of fluid are directed north and south across a latitude circle in any interval. On the average, heat is carried from warm areas to cool by an amount proportional to the gradient of the temperature:

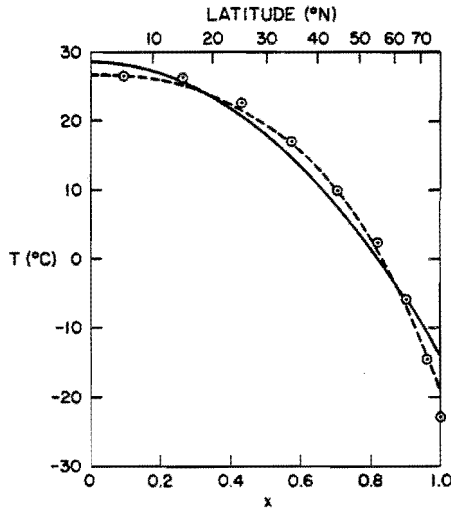$$\text{heat flux} \propto -C(1 - x^2)^{1/2} \, dT(x)/dx \qquad (20)$$

Fig. 5. Mean annual northern hemisphere zonally averaged temperature (degrees Celsius) versus sine of latitude for the two-mode approximation to the diffusive model (solid curve), the observations (circled dots), and a fit including $P_4(x)$ (dashed curve) [from *North*, 1975*b*] (cf. (32)).

where C is the heat capacity per unit area. The proportionality coefficient in this simple model would be a diffusion coefficient.

The amount of heat per unit time per unit area leaving a strip is the divergence of the flux which is proportional to $-\nabla^2 T$, or in our notation,

$$-\frac{d}{dx} D(1 - x^2) \frac{dT(x)}{dx} \qquad (21)$$

where D may be a function of x and must be thought of as a free parameter to be adjusted empirically.

Obviously, (21) represents a gross oversimplification of the transport process. The most evident omission is the mean circulation in both atmosphere and oceans. We shall consider more general models after first studying the model defined by (21). One advantage of the form (21) is that it corresponds to a physical analog, namely, heat conduction, and therefore physically realizable solutions are guaranteed. With transport the energy balance equation becomes

$$-\frac{d}{dx} D(1 - x^2) \frac{dT(x)}{dx} + A + BT(x) = QS(x)a(x, x_s) \qquad (22)$$

The boundary conditions for symmetric solutions are given by

$$-D(1 - x^2)^{1/2} \frac{dT(x)}{dx} \bigg|_{x=0,1} = 0 \qquad (23)$$

Note that the system is nonlinear because of the ice-albedo feedback. The nonlinearity leads to the multiple solutions that we have already encountered with the simpler models.

Before solving the nonlinear system, let us insert observed values of the co-albedo $a(x)$ in (22) and see how the computed temperature field compares with the fields shown in Figure 4. First, take D to be a constant independent of x. Since the Legendre polynomials are eigenfunctions of the diffusion operator,

$$-\frac{d}{dx}(1 - x^2) \frac{dP_n(x)}{dx} = n(n + 1)P_n(x) \qquad (24)$$

and since, individually, they satisfy the boundary conditions (23), the even-numbered $P_n(x)$ form a convenient basis set for expansions. Consequently, we expand the surface temperature

$$T(x) = \sum_{n(\text{even})} T_n P_n(x) \qquad (25)$$

and insert the expansion into the energy balance equation (22); multiply by $P_n(x)$ and integrate over all values of x from 0 to 1. Making use of the orthogonality relation

$$\int_0^1 dx \, P_n(x)P_m(x) = \frac{\delta_{mn}}{2n + 1} \qquad m, n \text{ (even)} \qquad (26)$$

we have

$$L_n T_n + \delta_{0n} A = QH_n \qquad (27)$$

where

$$L_n = n(n + 1)D + B \qquad (28)$$

and

$$H_n(x_s) = (2n + 1) \int_0^1 P_n(x)S(x)a(x, x_s) \, dx \qquad (29)$$

Even though we intend to use the observed $a(x)$, we have retained x_s in (29) for later applications. Since the $a(x)$ are given by (18), the H_n are determined, and as a result, (27) is easily solved:

$$T_n = QH_n/L_n - \delta_{0n} A/B \qquad (30)$$

For $n = 0$,

$$T_0 = (QH_0 - A)/B \qquad (31)$$

which is equivalent to (19). As before, T_0 is the planetary average temperature. The form of (31) holds not only for the diffusive transport (21) but also for any term that is the divergence of a flux which itself satisfies a zero condition at the endpoints (equator and pole). Using the coefficients specified earlier, we obtain, as before, $T_0 = 14.97°C$.

We turn now to $n = 2$. From (3) and (18) we compute $H_2 \cong -0.500$. In order to compute T_2 we must know D, which was left as an adjustable parameter. By taking the observed value for T_2 ($-28.0°C$) we compute $D = 0.649$ W m^{-2} °C^{-1},
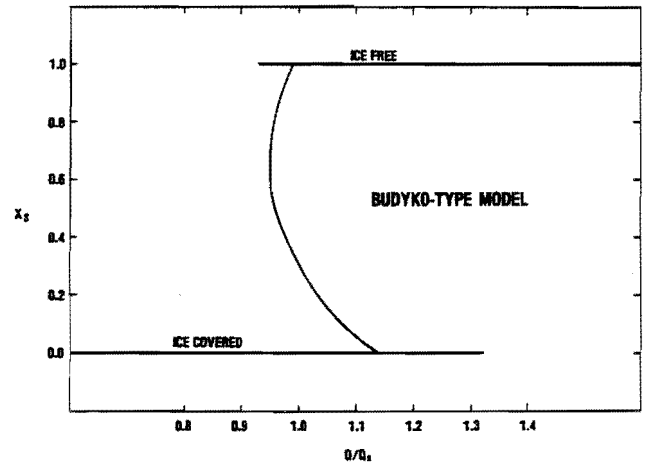

Fig. 6. Sine of steady state ice edge latitude x_s versus solar constant in units of its present value for the Budyko model; that is, the divergence of the horizontal heat flux is given by (33). The solution is given by (34).

or, in dimensionless form, $D/B = 0.310$. This approximation is called the two-mode or parabolic approximation to $T(x)$ [*Ångström*, 1928]:

$$T(x) \cong T_0 + T_2 P_2(x) \qquad (32)$$

It is plotted as the solid curve in Figure 5 along with the observations. Of course, the agreement shown in the figure does not confirm the model but rather illustrates how well a parabola fits the data.

Let us now consider $n = 4$. From observations [*Ellis et al.*, 1978] we obtain $H_4 = 0.022$, and using the previously computed value of D, we compute $T_4 = 0.5°C$. The observed value is $T_4 = -3.5°C$. The model gives a value that is almost an order of magnitude too small and has the wrong sign. In fact, the higher-mode amplitudes in the model are so small that the two-mode solution is close to the exact solution [*North*, 1975*b*]. Perhaps the most prominent feature of the observations that is not reproduced by the model is the flattening of $T(x)$ into a nearly isothermal band in the tropics. This flattening is probably due to mean motions in the tropical atmosphere (Hadley cell). The mean motions are more efficient than random motions at suppressing temperature deviations. *Lindzen and Farrell* [1977] have discussed methods of allowing for the tropical mean motions. Their motivation was based upon results derived from a more comprehensive model [*Schneider and Lindzen*, 1977] in which it was found that near the equator, $T(0) - T(x) \propto x^4$. In terms of the Legendre expansion, temperatures near the equator require contributions from $T_4 P_4(x)$. In an ad hoc way we can imitate the efficiency of thermal conduction in the tropics by allowing the diffusion coefficient to depend on x; for example, $D(x) = D_0 + D_2 P_2(x)$. There are then two free parameters, D_0 and D_2, that can be adjusted to give the observed values of T_2 and T_4. In agreement with Lindzen and Farrell we find $D(x)$ large near the equator and small near the pole [*North et al.*, 1977]. Although such tricks suffice to correct the value of T_4, other processes (such as varying relative humidity, lapse rates, and cloudiness) that would affect the infrared emission could also contribute to T_4. Further discussion of the limitations of the diffusive approximation are postponed to section 4.

Let us interpret the expansion (25). Each succeeding term in (25) contains information pertaining to smaller and smaller spatial scales. The first few terms give us the gross features of the planetary climate. T_0 is the planetary average; $\frac{1}{2}T_2$ is a rough measure of the pole-to-equator temperature difference; higher-order terms reveal features at finer spatial scales. Hence the spectral method of solving climate models provides a framework in which mathematical (or numerical) technique goes hand in hand with the concept of a model hierarchy discussed earlier.

The two-mode approximation just discussed was derived for diffusive heat transport with constant coefficient. The form of the transport, however, need not be restricted if (25) is truncated at $n = 2$. For example, instead of using the diffusive term (21), *Budyko* [1969] used

$$\gamma[T(x) - T_0] \qquad (33)$$

where γ is an empirical coefficient similar to D. Budyko's model is thus given by (22), with (33) replacing the first term. In the two-mode approximation the models are identical. By substituting (32) into (21) we obtain

$$6DT_2 P_2(x) = 6D[T(x) - T_0] \qquad$$

which is identical to (33) with $\gamma = 6D$. While the two models are identical in the two-mode approximation, they differ in higher modes.

Budyko's model can be solved analytically [*Chýlek and Coakley*, 1974] by roughly the same method we used for the no-transport model. After some straightforward algebra we obtain

$$Q(x_s) = \frac{A + (B + \gamma)T_s + \gamma A/B}{S(x_s)a_s + \gamma H_0(x_s)/B} \qquad (34)$$

Note that if $\gamma = 0$, (34) becomes the solution for the no-transport model (17). The solution curve for this version of the Budyko model is shown in Figure 6. The twigs at $Q/Q_0 = 0.99$ and 1.13 come about in the same way as in the no-transport model (Figure 3).

Although there is a closed form solution to Budyko's model, (34), it is instructive to investigate the spectral properties of the model. Expanding the temperature field as in (25) and inserting the expansion into the energy balance equation, we obtain again (27), but with L_n given by

$$L_n^B = \gamma + B - \delta_{n0}\gamma$$

In the diffusive model, $T_n \propto 1/L_n$, and thus if $D > 0$, the higher modes ($n > 2$) are strongly suppressed. In the Budyko model, on the other hand, the higher modes are not suppressed. As a result a discontinuity in $a(x, x_s)$ leads to a discontinuous temperature field in the Budyko model but not in the diffusive model.

The time dependence of these models also differs. If we add heat storage $C\, \partial T/\partial t$ to the energy balance equation and expand the temperature fields, then we obtain (27) with the additional term $C\dot{T}_n$ on the left-hand side. If the solar constant is suddenly switched off, the individual mode amplitudes decay exponentially with time constant C/L_n. In diffusive models, features or anomalies that have small spatial scales decay rapidly, whereas in Budyko-type models, small space scale features decay at the rate of the planetary scale features ($n = 2$).

Let us now consider some generalizations of the diffusive model in the two-mode approximation. Suppose D depends on latitude, $D(x) = \eta w(x)$. The $n = 0$ relation (31) is unaltered, and the $n = 2$ version of (30) is also unaltered provided we replace D in (28) by D_n', which for $n = 2$ is given by

$$D_2' = -5\eta \int_0^1 dx\, P_2(x) \frac{d}{dx}\left[(1 - x^2)w(x) \frac{dP_2(x)}{dx}\right] \qquad (35)$$

Since the integral in (35) is a constant, to be computed once and for all, it may be absorbed into the phenomenological constant η. The constant η is to be determined as before, so that in the two-mode approximation, $D(x) = \eta w(x)$ is formally equivalent to constant D [*North*, 1975*b*].

This formal equivalence is also retained for other transport models. For example, *Sellers* [1969] included a mean circulation term given by

$$\frac{V(x)}{R}(1 - x^2)^{1/2}\frac{dT(x)}{dx} \qquad (36)$$

where $V(x)$ is an empirically determined advective velocity field. As above, in the two-mode approximation this term may be absorbed into the constant D. Another form of interest is $K\nabla^4 T(x)$, which could occur as an added term in a turbulent (random) atmosphere model [*North*, 1976; *Kells*, 1976]. Be-
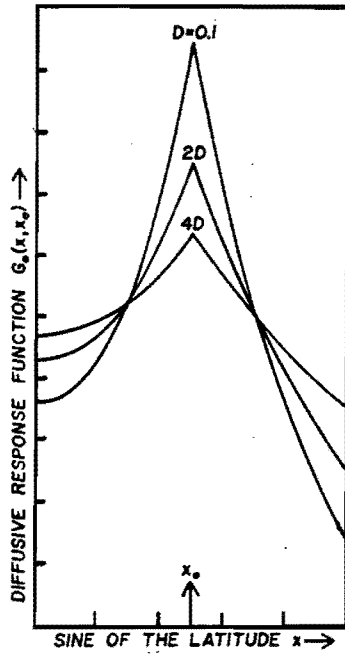
Fig. 7. The Green's function $G_0(x, x_0)$, defined by (40), (41), and (44), for the constant diffusion model versus sine of latitude x and for which a heat source is located at sine of latitude x_0. Note that smaller values of the diffusion coefficient D lead to a more localized response.

cause $\nabla^4 P_n(x) = [n(n + 1)]^2 P_n(x)$, the formal equivalence to constant diffusion in the two-mode approximations is maintained.

The formal equivalence of so many different models in the two-mode approximation explains why various published models give the same qualitative results. Of course, it is necessary that the two modes represent a suitable fit to observations. It is also necessary that the two-mode solution approximate the exact solution when the nonlinear ice-albedo feedback is included. To obtain an exact solution, we may solve the system (22) analytically. Here we retain the x_s dependence in $H_n(x_s)$ (equation (27)). Dividing (27) through by L_n, multiplying by $P_n(x_s)$, summing over n, and using (15), we obtain

$$A/B + T_s = Q \sum_{n(even)} [H_n(x_s)P_n(x_s)/L_n]$$

or

$$Q(x_s) = (A + BT_s) \left[B \sum_{n(even)} [H_n(x_s)P_n(x_s)/L_n] \right]^{-1} \quad (37)$$

These solutions have been given by *Held and Suarez* [1974] and by *North* [1975a, b].

Note that the formal solution (37) also holds for the Budyko model or even a $K\nabla^4 T$ model if the L_n are appropriately modified. Since it is formally correct for any $a(x, x_s)$, the solution is not restricted to a discontinuous albedo. We could use a smoothed albedo at the ice cap edge such as

$$a(x, x_s) = c_0 + c_1 \tanh [(x - x_s)/w] \quad (38)$$

as will be discussed later.

Generalized Treatment of Transport

To generalize (23), let the energy balance equation be given by

$$L[T] + A(x) = QS(x)a(x, x_s) \quad (39)$$

where L is a linear operator [*Cahalan and North,* 1979]. The model is completed by the ice line condition (15) and boundary conditions similar to (23). For constant diffusion,

$$L = -D \frac{d}{dx}(1 - x^2) \frac{d}{dx} + B \quad (40)$$

In general, however, L might include other integral or differential operators.

We shall assume that the Green's function $G_0(x, x')$ for L exists, so that

$$L_x G_0(x, x') = \delta(x - x') \quad (41)$$

where $\delta(x - x')$ is the Dirac delta function and the subscript x on L indicates that only the x variable is affected by L. The solution $J(x)$ to the linear inhomogeneous problem

$$L_x J(x) = \rho(x) \quad (42)$$

where $\rho(x)$ is a known function, is uniquely given by

$$J(x) = \int_0^1 G_0(x, x')\rho(x') \, dx' \quad (43)$$

provided L and the associated boundary conditions lead to a unique inverse. (For properties of L necessary for the existence and uniqueness of G_0, see, for example, *Courant and Hilbert* [1953].) The Green's function for constant diffusion is given by

$$G_0^D(x, x') = \sum_{n(even)} \frac{(2n + 1)P_n(x)P_n(x')}{L_n} \quad (44)$$

(A closed form expression for (44) is derived in Appendix A.)

For latitude-dependent diffusion

$$L^{D(x)} = -\frac{d}{dx} D(x)(1 - x^2) \frac{d}{dx} + B \quad (45)$$

we use the eigenfunctions $f_n(x)$, defined by

$$-\frac{d}{dx} \left[D(x)(1 - x^2) \frac{df_n(x)}{dx} \right] = \mu_n f_n(x) \quad (46)$$
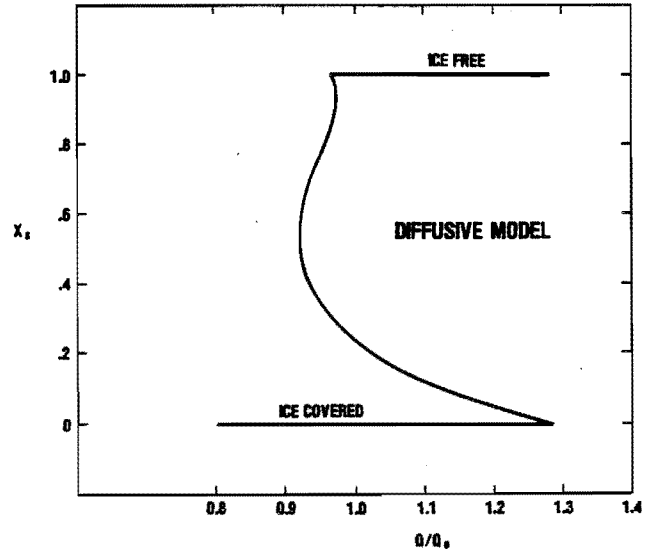

Fig. 8. Same as Figures 3, 5, and 6 except that the model employs diffusive heat transport. The model is defined by (15), (22), and (23) with the analytical solution given by (37).

where the μ_n are eigenvalues. The system (46) forms a Sturm-Liouville system [*Courant and Hilbert*, 1953], provided $D(x) > 0$ and is well behaved. The $f_n(x)$ are proportional to $P_n(x)$ for $D = $ const. The $f_n(x)$ also are orthogonal and can be normalized such that

$$\int_0^1 dx\, f_m(x)\, f_n(x) = \delta_{mn} \tag{47}$$

Furthermore, the lowest eigenvalue $\mu_0 = 0$ and $f_0(x) = 1$ and, for $n \to \infty$, $\mu_n \propto n^2$. The Green's function for the system is given by

$$G_0{}^{D(x)}(x, x') = \sum_n f_n(x) f_n(x')/l_n \tag{48}$$

where $l_n = \mu_n + B$.

The Green's function $G_0(x, x_0)$ may be interpreted as the thermal response of the model to a localized heat source at $x = x_0$. Figure 7 shows a graph of this function for the constant D diffusion model. For large D the heat is smeared out; for D tending to zero the response tends to a spike at $x = x_0$. One important feature, to be used later, is that $G_0(x, x_0)$ is positive definite.

The formal solution of any model possessing a Green's function is straightforward. Using (42) and (43), we convert (39) to the integral equation

$$T(x) = \int G_0(x, x')[QS(x')a(x', x_s) - A(x')]\, dx' \tag{49}$$

As before, we satisfy the ice line condition (15) by setting $x = x_s$ in (49). Solving for Q, we obtain

$$Q(x_s) = \frac{T_s + \int_0^1 G_0(x_s, x')A(x')\, dx'}{\int_0^1 G_0(x_s, x')S(x')a(x', x_s)\, dx'} \tag{50}$$

This solution reduces to the special cases (34) and (37) when the appropriate substitutions are made.

Figure 8 shows the $Q(x_s)$ versus x_s curve for the constant D diffusion model, computed by using (37) with terms through $n = 6$. (Note that in Figure 8, Q is normalized to Q_0.) The exact solution [*North*, 1975a] differs little from that shown in Figure 8. The most striking difference between the diffusive model and the Budyko model is that the twigs in the Budyko model split open into two branches in the diffusive model. Just below $x_s = 1$ the slope changes sign, and dx_s/dQ tends to zero at the cusp where the two branches meet [*Drazin and Griffel*, 1977; *Cahalan and North*, 1979]. If Q is increased quasi-statically from Q_0, Figure 8 indicates that the ice cap first shrinks to the point where the slope changes sign, and beyond that presumably a jump to an ice-free earth occurs. Let us examine whether this sign change and the associated cusp are physically realistic. *Lin* [1978] and *North* [1975b] noted that because series (25) converges rapidly, models with nonlinear diffusion coefficient ($D \propto dT/dx$) are easily solved. The two-mode results for the nonlinear model are virtually identical with those for the linear model, but retention of the higher modes in the nonlinear model removes the cusp at $x_s = 1$ shown in Figure 8. A picture more like Figure 6 emerges.

The cusp can also be removed by smoothing the albedo at the ice line. *Cahalan and North* [1979] have experimented with the smoothed form (38), choosing C_1 and C_2 to match the val-

ues of the corresponding step albedo but allowing w, a measure of the smoothing width, to differ from zero. As the width of the smoothing increases, the cusp disappears, and eventually, the slope becomes positive near $x_s = 1$. *Coakley* [1979] also mentions this effect. For smooth albedo the twig in the Budyko model at $x_s = 1.0$ is also removed. Cahalan and North have shown that such behavior follows generally from (49) and (50). We must conclude that the appearance of the twig or cusp near $x_s = 1$ in the simple models is probably unphysical and merely an artifact of the mathematically convenient but physically unrealistic step function albedo.

3. SEASONAL MODELS

In extending the one-dimensional climate model to include seasonal cycles we wish to study the sensitivity of the model to see if it differs from that of the corresponding mean annual model. In other words, do seasonal changes affect the mean annual climate?

There have been several attempts at developing seasonal models, notably the energy balance models developed by *Adem* [1962] and *Sellers* [1973] and the general circulation models developed by Manabe and his co-workers [*Wetherald and Manabe*, 1972; *Manabe et al.*, 1979]. More recently, there have been studies by *Thompson and Schneider* [1979], who seasonalized the Gal-Chen/Schneider version of the Sellers model [*Schneider and Gal-Chen*, 1973; *Gal-Chen and Schneider*, 1976]; *Ramanathan et al.* [1979], who seasonalized the Budyko model; and *North and Coakley* [1978, 1979], who seasonalized the simple diffusive model [*North*, 1975a, b]. The model studies so far have similar qualitative conclusions, so that it will suffice here to study the diffusive model as an example.

As before, the method of solution (Legendre polynomial expansion) is intimately connected with the philosophy of the model hierarchy approach. The development of the diffusive seasonal model is similar in spirit to the approach taken some time ago by *Fritz* [1960]. Our emphasis here will be on using the model to understand the main features of the seasonal cycle. As far as possible we will use analytical methods.

We begin by examining seasonal data for the zonally averaged temperature $T(x, t)$, the infrared flux $I(x, t)$, the co-albedo $a(x, t)$, and the heat per unit area reaching the top of the atmosphere, $QS(x, t)$. *North and Coakley* [1978, 1979] have shown that a convenient representation of the fields is first to symmetrize them so that data from only one hemisphere is used; the other hemisphere is given the same data but lagged by 6 months. After symmetrization the data are fitted to simple formulae

$$F(x, t) = F_0 + (A_{11} \cos 2\pi t + B_{11} \sin 2\pi t)P_1(x) + F_2 P_2(x) \tag{51}$$

where $F(x, t)$ can be any of the four fields. Each field is then characterized by the four coefficients in (51). Note that the mean annual fields are characterized by F_0 and F_2, while the amplitude and phase of the seasonal cycle may be computed from A_{11} and B_{11}. Fits for the four fields using the symmetrized northern hemisphere (SN), symmetrized southern hemisphere (SS), and global data have been performed by *North and Coakley* [1979]; results for SN are listed in Table 1. Figures 9–12 show examples of the curves for various seasons along with observations. From the curves we see that (51) captures the gross features of the fields but misses the fine structure, which is particularly noticeable at low latitudes. In keeping with the approach taken so far in this review we would not

TABLE 1. Expansion Coefficients for Equation (52) for the Symmetrized Northern Hemisphere Fields

Field	F_0	A_{11}	B_{11}	F_2	E_{rms}
$T(x, t)$	14.9	−13.2	−8.1	−28.0	2.0
$I(x, t)$	234.4	−33.7	−17.7	−55.6	9.5
$\alpha(x, t)$	31.9	7.2	5.4	20.2	2.6
$S(x, t)$	1.000	−0.796	0.006	−0.477	0.056

$T(x, t)$ is sea level temperature (degrees Celsius), $I(x, t)$ is infrared radiation to space (watts per square meter), and $\alpha(x, t)$ is albedo (percent). Also shown is $S(x, t)$, the normalized calculated solar energy reaching the top of the atmosphere. E_{rms} is the rms error associated with the fit [North and Coakley, 1979].

expect simple models to work on scales beyond $P_2(x)$ in (51). Indeed, attempts by North and Coakley to go beyond this mode failed.

As in the mean annual models, we adopt the Budyko form for the emitted infrared radiative flux,

$$I(x, t) = A + BT(x, t) \qquad (52)$$

With $A = 203.3$ and $B = 2.09$ W m^{-2} °C^{-1} [North and Coakley, 1979], (52) gives the best fit to the mode amplitudes listed in Table 1 for the emitted fluxes and temperatures of the northern hemisphere. The fit to observations is shown in Figure 10.

We construct the seasonal model along the lines of previous sections. In the seasonal model, however, a storage term $C(x, \phi) \partial T/\partial t$, must be added; $C(x, \phi)$ is a latitude- and longitude-dependent heat capacity per unit area. The forcing is given by the four amplitudes in the mode expansion of $S(x, t)$. The seasonal response is represented by the four amplitudes in the mode expansion of $T(x, t)$. A linear climate model would connect these two fields with a four-by-four response matrix. Linearity is suggested by the absence of higher harmonics in both the forcing and the response fields [North and Coakley, 1979]. The most general linear model with four components consists of a response matrix with 16 independent components. We shall see that most of these elements may be taken to be zero.

With the storage term added the energy balance model becomes

$$C(x, \phi)(\partial T/\partial t) - D\nabla^2 T + A + BT = QS(x, t)a(x, t) \qquad (53)$$

As an idealization of the northern hemisphere we take a single continent with coastlines running along meridians and with an area spanning 40% of each latitude belt. We separate the continent from the oceans because $C(x, \phi)$ is only about $0.16B$ years (C_L) over land and about $4.7B$ years (C_W) over the ocean mixed layer (75 m).

If (53) is integrated around a latitude belt, we obtain for the landmass (after dividing through by f_L, the fraction of land area)

$$C_L \frac{\partial T_L(x, t)}{\partial t} - D \frac{\partial}{\partial x}(1 - x^2) \frac{\partial}{\partial x} T_L - \frac{D_0}{f_L} \left. \frac{\partial T}{\partial \phi} \right|_{right}^{left}$$

$$+ A + BT_L = QS(x, t)a_L(x, t) \qquad (54)$$

where T_L is defined as the average temperature over land in a latitude belt. The gradient term is the difference between land and water temperatures divided by an effective angular distance over which the temperature change effectively occurs. The whole term may be written as

$$(v/f_L)(T_L - T_w) \qquad v > 0 \qquad (55)$$

where v is a new adjustable parameter that accounts for the land-sea interaction.

An equation analogous to (54) can be derived for $T_w(x, t)$, the temperature over oceans. The zonal average field is the weighted average given by

$$T(x, t) = f_L T_L + f_w T_w \qquad (56)$$

This kind of decomposition was first used by Sellers [1973].

If we substitute the truncated Fourier-Legendre series (51) for T_L and T_w into the resulting equations, we obtain

$$A + BT_0 = QH_0 \qquad (57)$$

$$C_{L,w} \frac{dT_1^{L,w}}{dt} + (2D + B)T_1^{L,w} + \frac{v}{f_{L,w}}(T_1^{L,w} - T_1^{w,L}) = QH_1 \qquad (58)$$

$$(6D + B)T_2 = QH_2 \qquad (59)$$

SYMMETRIZED NORTHERN HEMISPHERE SURFACE TEMPERATURE
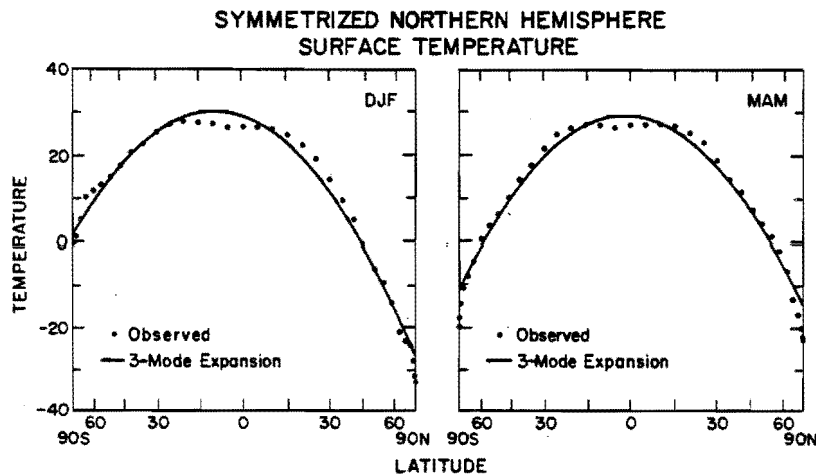
Fig. 9. Observed surface temperature of the symmetrized northern hemisphere (circles) and the representation of the surface temperatures obtained with the 00, 11, and 20 modes listed in Table 1 (solid curves). The surface temperatures are for northern hemisphere winter (December, January, and February (DJF)) and spring (March, April, and May (MAM)), but because the temperature fields have been symmetrized, the temperatures for summer and fall are obtained by reversing the abscissas [North and Coakley, 1979].

SYMMETRIZED NORTHERN HEMISPHERE INFRARED FLUX

Fig. 10. Observed infrared fluxes emitted by symmetrized northern hemisphere (circles) and the representation obtained with the 00, 11, and 20 modes listed in Table 1 (solid curves). The dashed curves show the fit obtained by using the 00, 11, and 20 modes of the temperature field (Table 1) in (53) [*North and Coakley*, 1979].

where

$$H_0(t) = \tfrac{1}{2}\{2a_0 + a_1(t)S_1(t)G_{011} + a_2S_2G_{022} + \cdots\} \quad (60)$$

$$H_1(t) = \tfrac{1}{2}\{a_0S_1(t)G_{101} + a_1(t)G_{110}$$
$$+ a_2S_1(t)G_{121} + a_1(t)S_2G_{112} + \cdots\} \quad (61)$$

$$H_2(t) = \tfrac{1}{2}\{a_2G_{220} + a_0S_2G_{202} + a_2S_2G_{222}$$
$$+ a_1(t)S_1(t)G_{211} + \cdots\} \quad (62)$$

and

$$G_{ijk} = \int_{-1}^{1} P_i(x)P_j(x)P_k(x)\, dx \quad (63)$$

The relevant coupling coefficients G_{ijk} are $G_{011} = \tfrac{2}{3}$, $G_{022} = \tfrac{2}{3}$, $G_{121} = \tfrac{4}{15}$, and $G_{222} = \tfrac{4}{35}$. In (60)–(62), $S_0 = 1$; $a_1(t)$ and $S_1(t)$ represent the first-harmonic contributions to the coefficients of $P_1(x)$ in the expansions of $a(x, t)$ and $S(x, t)$. For simplicity we have assumed the co-albedos for land and ocean areas to be the same. Also for simplicity we take H_0 and H_2 to be independent of time. We do so by replacing $a_1(t)S_1(t)$ by its annual average and by neglecting second-harmonic contributions.

We see that (57) and (59) are just the equations for the two-mode approximation to the mean annual model. The only

new contributions to these equations are the terms proportional to $a_1(t)S_1(t)$. These terms are called 'residuals.' In T_0 this term causes a warming of about 2°C that is not present in the mean annual models. The residual occurs because the northern hemisphere is more reflective in winter than in summer (making the seasonal amplitude larger), but the impact of absorption in summer is greater because the sun is low in the sky during winter. This residual was noted by *Wetherald and Manabe* [1972] in their study of the seasonal cycle with a GCM.

The seasonal amplitude of the zonal average surface temperature may be obtained by solving (58) for land and ocean masses and reconstructing $T_1(t)$ from (57). The amplitude of $T_1(t)$ for the northern hemisphere is 15.5°C; the phase lags the solar heating by 32 days. For reasonable values of the parameters [*North and Coakley*, 1978, 1979] (that is, D taken from the mean annual model; ν very nearly zero; C_L, C_w computed heat capacities for a column of air and a column of ocean mixed layer (75 m); and $f_L = 0.40$) the model yields the correct phase and amplitude for the seasonal mode. (Note that in this section, as in the work by *North and Coakley* [1979], we have used $Q = 340$ W m^{-2}, whereas in section 2 we used 335 W m^{-2}.)

SYMMETRIZED NORTHERN HEMISPHERE ALBEDO

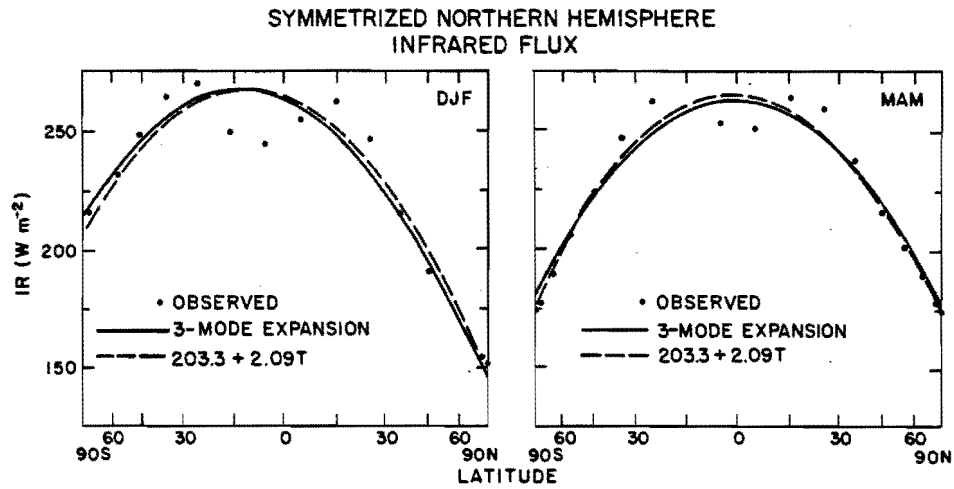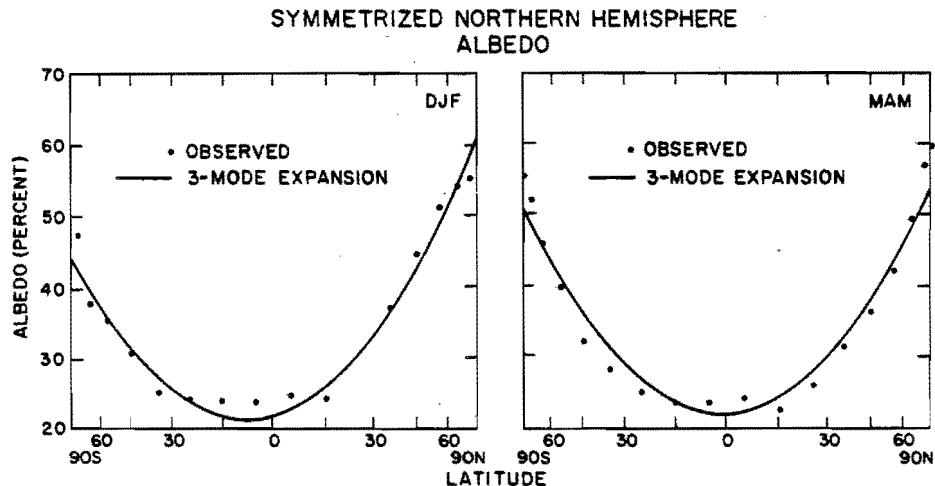Fig. 11. Observed albedo of the symmetrized northern hemisphere (circles) and the representation of the albedo obtained with the 00, 11, and 20 modes listed in Table 1 (solid curves) [*North and Coakley*, 1979].
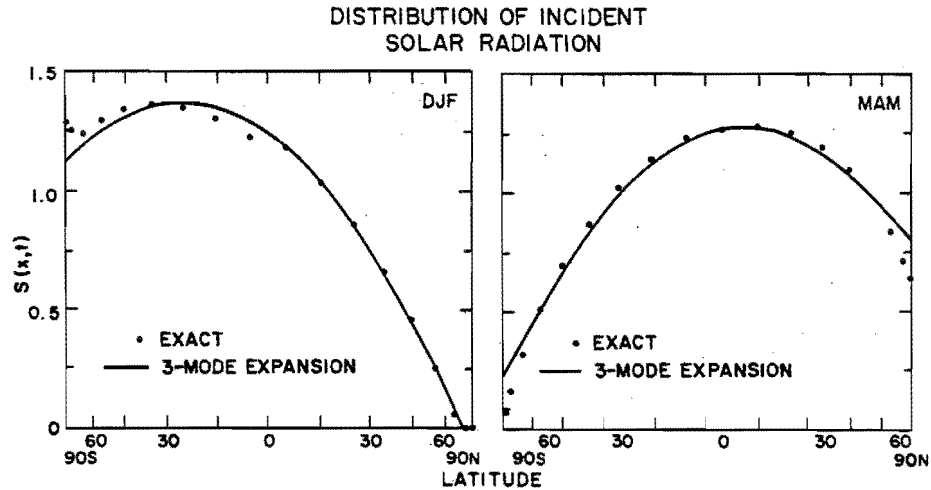
DISTRIBUTION OF INCIDENT
SOLAR RADIATION

Fig. 12.   Distribution of incident solar radiation (circles) and the representation of the distribution obtained with the 00,
11, and 20 modes listed in Table 1 (solid curves) [North and Coakley, 1979].

Simple experiments with the solutions show that the amplitude and phase are rather sensitive to the fraction of land, f_L. For instance, if f_L is reduced to 0.20 (southern hemisphere), then the seasonal amplitude is reduced to about 8°C, in rough agreement with the symmetrized southern hemisphere data.

It is possible to parameterize $a(x, t)$ in the model in terms of a snow line (or cloud line) attached to an isotherm and thereby produce a self-consistent feedback scheme. In order to study climate change or sensitivity, North and Coakley [1979] have considered an ice cap whose edge is at the mean annual −10°C isotherm and a seasonally moving snow line on land whose edge is at the instantaneous 0°C isotherm. The resulting energy balance model is slightly nonlinear, and the four coefficients in (51) for $T(x, t)$ are obtained by iterating a system similar to (57)–(59). The results indicate that this model has about the same sensitivity to solar constant changes as the corresponding mean annual model. The small (few percent) differences can be explained in terms of changes in the residuals discussed earlier.

4. SENSITIVITY AND THE PARAMETERIZATIONS

In the preceding sections we introduced simple climate models and gave a short survey of solvable examples. The primary purpose of these models is to guide our understanding of climate feedback mechanisms. We must view with skepticism, however, the numerical results obtained with the simple models. These results are bound to be sensitive to the various parameterizations used to link the energy fluxes to surface temperatures. In this section we discuss the most commonly used parameterizations, how they were developed, how reliably they reproduce the relationships between the fluxes and the surface temperatures, and, finally, how they influence the fundamental sensitivity of the model as given by the sensitivity parameter β_0.

To understand how the parameterizations affect β_0, we note that the sensitivity for a global model may be derived directly from the condition of global energy balance [Cess, 1976; Lian and Cess, 1977]:

$$I_0 = QH_0(T_0) \qquad (64)$$

Differentiating (64), we obtain

$$\beta_0 = Q\,\frac{dT_0}{dQ} = \frac{I_0}{(dI_0/dT_0) - Q(dH_0/dT_0)} \qquad (65)$$

Obviously, β_0 is influenced by the sensitivity of the infrared radiative flux to changes in the surface temperature, dI_0/dT_0; it is also influenced by the sensitivity of the planetary albedo to changes in surface temperature, $Q\,dH_0/dT_0$, the albedo-temperature feedback. Less obvious, however, is the influence of the meridional transport on β_0. The meridional transport affects β_0 primarily through its influence on the albedo-temperature feedback. If, for example, the surface albedo is taken to be a function of the local surface temperature, then H_0 will be a function of the latitudinal distribution of temperature, which in turn is governed by the meridional transport. As a result the albedo-temperature feedback is subject to both the albedo parameterization and the transport parameterization.

Note that here we are considering only the uncertainty in the sensitivity due to a small global change in solar input. As we have seen, for larger changes a critical solar constant is reached beyond which only ice-free or ice-covered steady states exist. As was emphasized by Warren and Schneider [1979], uncertainties in β_0 lead to large uncertainties in this critical value. In simple models, reductions in β_0 tend to be as-
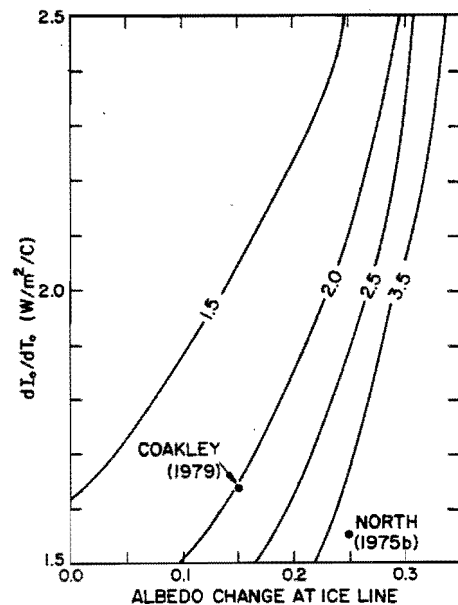

Fig. 13.   Isopleths of the decrease in global average temperature calculated for a 1% decrease in the solar constant [Coakley, 1979].

sociated with lower critical points, as is illustrated in Figures 13 and 14, but even this correlation could be reversed by neglected nonlinear effects. In section 7 we consider small local changes in heating and an associated latitude-dependent sensitivity. Again, any uncertainty in β_0 contributes to a large uncertainty in this spatial sensitivity. In the following discussion we consider uncertainties in the infrared, co-albedo, and transport parameterizations and their effect on β_0.

Infrared Parameterization

A method of parameterization commonly used in energy balance climate modeling was first applied by *Budyko* [1969] to obtain the emitted flux in terms of the surface temperature. He hypothesized that the way meteorological variables influence the flux is exhibited in latitudinal and seasonal climatological data. To obtain the relationship, he collected meteorological records from a variety of stations in the northern hemisphere, and with these records he calculated the emitted IR flux at the top of the atmosphere. From the results of these calculations he deduced that the emitted flux is given by

$$I = A_1 + A_2 A_c + (B_1 + B_2 A_c)T \qquad (66)$$

where A_1, A_2, and B_1, and B_2 are constants, A_c is the cloud cover fraction, and T is the surface temperature. *Cess* [1976] applied (66) to climatological records of zonal mean surface temperatures, cloud cover, and satellite-observed emitted fluxes. He found that (66) indeed provided an excellent fit to the climatological data. For each 10° latitude zone, with $A_1 = 257$ W m^{-2}, $A_2 = -91$ W m^{-2}, $B_1 = 1.63$ W m^{-2} °C^{-1}, and $B_2 = -0.11$ W m^{-2} °C^{-1} the parameterization fits the northern hemisphere data with a maximum error of 1.2% of the emitted flux. With $A_1 = 262$ W m^{-2}, $A_2 = -81$ W m^{-2}, $B_1 = 1.64$ W m^{-2} °C^{-1}, and $B_2 = -0.09$ W m^{-2} °C^{-1} the parameterization fits the southern hemisphere data with a maximum error of 2.3%.

Despite the different climates exhibited by the hemispheres the parameterization proved successful at fitting the observations, the constants changing only slightly from one hemisphere to the other. Such results argue for the universality of the parameterization. Most remarkable is that because $B_2 A_c \ll B_1$ for both hemispheres, $B_1 = dI_0/dT_0$ is the only parameter, according to (65), that would affect β_0, and it is the same (1.6 W m^{-2} °C^{-1}) for both hemispheres. The somewhat larger value of $B = 2.09$ W m^{-2} °C^{-1} used in earlier sections for illustrative purposes arises from applying $I = A + BT$ to the zonal climatological data and ignoring cloud cover. Also ignoring cloud cover, *Oerlemans and Van den Dool* [1978] obtained 2.23 W m^{-2} °C^{-1}.

Sellers [1969] developed another parameterization for the emitted flux. It is nonlinear in surface temperature. *North* [1975b], however, showed that when the parameterization is linearized, it resembles the Budyko parameterization with constants that differ only slightly from those given by Budyko.

That the emitted IR flux is so simply related to surface temperatures seems miraculous when we consider that the earth's surface and each segment of the atmosphere contributes to the emitted flux. The contribution made by a segment of the atmosphere depends on its temperature and concentration of emitters. Water vapor and clouds are the major emitters. As clouds and water vapor are confined to the troposphere and as tropospheric temperatures are sufficiently high, most of the IR flux emanating from the atmosphere is emitted by the troposphere. Thus any feedbacks that link surface temperature to
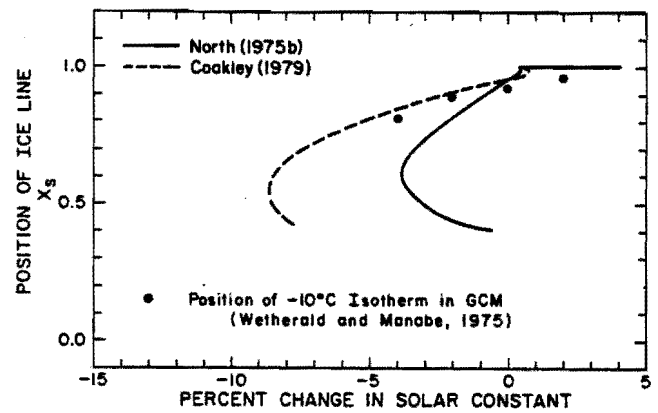

Fig. 14. Equilibrium position of the ice line (-10°C isotherm) as a function of the solar constant. Results obtained with radiation parameterizations adopted by *North* [1975b] (solid curve) and by *Coakley* [1979] (dashed curve). For comparison the positions of the -10°C isotherm of the lowest GCM level from calculations performed by *Wetherald and Manabe* [1975] are represented by circles [*Coakley*, 1979].

tropospheric temperature profiles, humidity, or cloud cover are likely to influence the sensitivity of the outgoing flux to changes in surface temperature.

To illustrate how various feedbacks might affect β_0, we take dI_0/dT_0 to be given by [*Coakley*, 1977]

$$\frac{dI_0}{dT_0} = \frac{\partial I_0}{\partial T_0} + \frac{\partial I_0}{\partial A_c}\frac{dA_c}{dT_0} + \frac{\partial I_0}{\partial T_c}\frac{dT_c}{dT_0} + \frac{\partial I_0}{\partial \Gamma}\frac{d\Gamma}{dT_0} \qquad (67)$$

In (67) dA_c/dT_0 represents the rate of cloud amount change with surface temperature change, the cloud amount feedback; dT_c/dT_0 the cloud top temperature feedback; and $d\Gamma/dT_0$ the tropospheric lapse rate feedback. The partial derivatives in (67) are evaluated while keeping the remaining variables fixed.

Feedbacks with the largest potential influence on dI_0/dT_0 are those related to cloud cover. *Cess and Ramanathan* [1978] report that $-91 < \partial I_0/\partial A_c < -34$ W m^{-2}, depending on how the vertical profile of cloud cover changes as the total amount of cloud cover changes. We note then that a cloud amount feedback $dA_c/dT_0 = 0.02$°C^{-1} would contribute as much as 1.8 W m^{-2} °C^{-1} to dI_0/dT_0. That is, its contribution would be as large as the value deduced for dI_0/dT_0 from climatological records. Clearly, cloud amount feedbacks could greatly influence the sensitivity of the climate.

Another cloud-related feedback is the cloud top temperature feedback. Calculations made with globally averaged vertical column models of the earth's atmosphere [*Ramanathan and Coakley*, 1978] indicate that for fixed cloud top temperatures, $\partial I_0/\partial T_0 = 2.16 - 1.75A_c$, or 1.29 W m^{-2} °C^{-1} for $A_c = 0.5$, while for fixed cloud top altitude and constant tropospheric lapse rate ($dT_c/dT_0 = 1.0$), $\partial I_0/\partial T_0 + \partial I_0/\partial T_c(dT_c/dT_0) = 2.16 + 0.19A_c$, or 2.26 W m^{-2} °C^{-1} for $A_c = 0.5$. Thus dI_0/dT_0 could change by 1.0 W m^{-2} °C^{-1} if the cloud tops change from maintaining constant cloud top temperatures to maintaining constant cloud top altitudes. How the clouds might change during a climate change, however, remains a mystery.

The preceding values for dI_0/dT_0 were computed by assuming that the atmosphere maintains constant profiles of relative humidity. Thus as the tropospheric temperature increases, the concentration of water vapor is assumed to increase. The assumption is based on the observation that the earth's atmosphere appears to conserve relative humidity [*Manabe and*

Wetherald, 1967]. Global circulation models of the earth's atmosphere also seem to conserve relative humidity [*Manabe and Wetherald*, 1975; *Wetherald and Manabe*, 1975]. If, on the other hand, the atmosphere maintained profiles of constant absolute humidity, $dI_0/dT_0 = 3.7$ W m^{-2} °C^{-1} under the conditions of fixed cloud top altitude [*Ramanathan and Coakley*, 1978]. We note then that without the observed moisture feedback affecting the opacity of the atmosphere, the emitted radiation exhibits the sensitivity of a blackbody at the earth's equivalent temperature $T_e = 254$ K.

Finally, as with the moisture and the cloud cover feedbacks, lapse rate feedbacks are also expected to influence dI_0/dT_0. *Ramanathan* [1977] noted that in the 0–2% solar constant change experiments performed with a GCM [*Wetherald and Manabe*, 1975], dI/dT with fixed cloud top altitude ranged from $2.4 + 1.45A_c$ near the equator to $1.7 - 0.81A_c$ near the pole. He attributed the range to differences in lapse rate changes. Near the equator, moist adiabatic adjustment governed the lapse rate changes, while near the pole a mixture of radiative and advective processes governed the lapse rate changes.

Obviously, the feedbacks mentioned thus far could have a profound influence on dI_0/dT_0 and thereby on β_0. How these feedbacks work and what other feedbacks might affect the climate sensitivity represent the focus of much ongoing research. Given the range of possibilities illustrated thus far, it is difficult to specify a probable range for dI_0/dT_0. Barring cloud amount changes, however, we might accept the range from 1.3 W m^{-2} °C^{-1}, obtained with fixed relative humidity, lapse rate, and cloud top temperature, to 3.1 W m^{-2} °C^{-1}, obtained with fixed relative humidity, cloud top altitude, and moist adiabatic adjustment exhibited in the tropical region by the GCM.

In accepting this range we should note that contrary to the finding by Budyko and Cess of a universal constant for B_1, experiments with a GCM indicate that dI/dT changes with latitude. Oddly enough, the Budyko parameterization fits the zonal climatology of the GCM about as well as it does the earth's [*Coakley and Wielicki*, 1979]. The apparent discrepancy is resolved when we recognize that the feedbacks that influence the climate change exhibited by the GCM are not revealed by applying (66) to the zonal fields. In a similar way we might expect that application of (66) to the earth's fields would also miss the feedbacks that could significantly affect climate change.

Albedo Parameterization

As the earth cools, we expect the extent of permanent ice and snow cover to increase, thereby increasing the earth's albedo. To simulate this effect, *Budyko* [1969] proposed the simple mechanism introduced in section 2. Poleward of the −10°C mean annual isotherm the surface is to be covered with ice; equatorward it is to be ice free. The −10°C isotherm represents the boundary of permanent ice and snow cover for the northern hemisphere. Budyko assigned albedos of 0.62 for ice-covered regions and 0.32 for ice-free regions. Hence the albedo change is 0.3 when the surface changes from being ice covered to ice free. As is indicated in Figures 13 and 14, such a large change in the albedo at the ice line makes the model highly sensitive to solar constant changes and causes it to produce the completely ice-covered solution when the solar constant is only slightly reduced.

Lian and Cess [1977] noted, however, that because of the zenith angle–dependent reflectivities of clouds and surfaces, al-

bedos of the ice-free regions will be high at high latitudes because of large zenith angles and low at low latitudes. As a result the change in albedo as the surface changes from ice-free to ice-covered conditions will be large at low latitudes but small at high latitudes, where the ice cover changes take place. Allowing for the zenith angle–dependent reflectivities referred to by Lian and Cess, *Coakley* [1979] finds that the change in albedo at the ice line is reduced to 0.15, for which $Q\, dH_0/dT_0 = 0.4$ W m^{-2} °C^{-1} under the current climatic conditions.

Instead of an ice line, *Sellers* [1969] allowed for the change in albedo by taking

$$\begin{aligned} \alpha &= b + cT & T &< 283.16 \\ \alpha &= b - 2.55 & T &\geq 283.16 \end{aligned} \tag{68}$$

From albedos and temperatures in the same latitude zones of the two hemispheres he deduced that $c = -0.009$ K^{-1}. He then made b a function of latitude so that (68) matched observed albedos.

Because of the zenith angle–dependent reflectivities noted by Lian and Cess, however, we would expect c to be a function of latitude and not a constant. From climatological observations of zonal albedos and surface temperatures, they deduce that c ranges from 0.0 K^{-1} for latitudes equatorward of 40°N (near the position of the +10°C isotherm and in agreement with (68)) to −0.0145 K^{-1} at 85°N. Using the latitude-dependent c, they obtain $Q\, dH_0/dT_0 = 0.3$ W m^{-2} °C^{-1}, while using the same model but with $c = -0.009$ K^{-1} at all latitudes, they obtain $Q\, dH_0/dT_0 = 1.0$ W m^{-2} °C^{-1}. This difference more than doubles the sensitivity of the model.

As with the emitted radiation, water vapor strongly influences the absorbed solar radiative flux. For fixed relative humidity, absorption by water vapor increases as the tropospheric temperature increases. *Coakley and Wielicki* [1979] estimate that for fixed relative humidity the change in absorption by water vapor contributes 0.2 W m^{-2} °C^{-1} to $Q\, dH_0/dT_0$.

Of the solar radiation reflected by the earth, clouds reflect between 70 and 80%. We would expect therefore that cloud amount feedbacks would strongly affect the sensitivity of the absorbed solar radiative flux to changes in surface temperature. For global average conditions [*Cess*, 1976],

$$Q\, \partial H_0/\partial A_c = Q(\alpha_s - \alpha_c) \tag{69}$$

where $\alpha_s = 0.18$ is the albedo for cloud-free regions and $\alpha_c = 0.43$ is the albedo for cloud-covered regions. Hence $Q\, \partial H_0/\partial A_c = -85$ W m^{-2}, and thus $dA_c/dT = 0.01$°C^{-1} is sufficient to swamp the feedbacks examined so far.

Clearly, the cloud amount feedback could strongly influence the sensitivity of the albedo to changes in surface temperature, just as it could strongly influence the sensitivity of the emitted IR flux. We note, however, that the change in the absorbed solar radiative flux caused by a change in cloud cover is somewhat compensated for by the change in the emitted IR flux. That is, the term in the denominator of (65) contributed by a cloud amount feedback, $(\partial I_0/\partial A_c - Q\, \partial H_0/\partial A_c)\, dA_c/dT_0$, is smaller than either $\partial I_0/\partial A_c(dA_c/dT_0)$ or $Q\, \partial H_0/\partial A_c(dA_c/dT_0)$. In fact, it may be negligible [*Cess*, 1976]. Its magnitude, however, is the focus of considerable debate [*Cess and Ramanathan*, 1978; *Ohring and Clapp*, 1980; *Hartmann and Short*, 1980].

Barring again cloud amount feedbacks, we might accept a range from $Q\, dH_0/dT_0 = 0.2$ W m^{-2} °C^{-1} for fixed relative

humidity and no ice-albedo feedback to 0.6 W m^{-2} °C^{-1} for fixed relative humidity with ice-albedo feedback. The larger values obtained with the Budyko and Sellers parameterizations appear unwarranted in view of the zenith angle–dependent reflectivity corrections which they neglect.

Transport

In the two-mode approximation the sensitivity of simple models was shown in section 2 to be unaffected by the model used for the meridional transport. *Held and Suarez* [1974], *North* [1975b], and *Lin* [1978] have also shown that various diffusion parameterizations that are nonlinear in the meridional temperature gradient, such as the parameterization suggested by *Stone* [1973], also have relatively little effect on sensitivity. If a third mode is added, then corrections to β_0 of the order of $T_4/T_2 \sim 10\%$ are to be expected. Allowing for a Hadley cell along the lines suggested by *Lindzen and Farrell* [1977], for example, might be expected to make such a correction.

Remember that in the simple models the transport only affects β_0 indirectly. The transport enters the energy balance as the divergence of a heat flux, and integrals over the globe to obtain the global energy budget cause the transport term ($-R^2 D\nabla^2 T$ or $\gamma(T - T_0)$) to disappear from the global energy balance (64); consequently, because dI_0/dT_0 is usually taken to be constant, the transport can influence the sensitivity only through its impact on the albedo-temperature feedback $Q \, dH_0/dT_0$. Without albedo-temperature feedback the meridional transport could have no influence on the sensitivity of these simple models.

A realistic model for the transport has yet to be constructed. In an attempt to check the diffusion mechanism, *Lorenz* [1979] has recently made a study of sensible heat transport in the real atmosphere. He finds that diffusion parameterizations may work for the largest scales (Legendre index $n = 0$, 1, 2) but surely fail for smaller scales (flux and temperature gradient are improperly correlated).

Despite the omnipresence of diffusive transport models, the results of the GCM referred to earlier suggest that its transport remains constant independent of surface temperature and regardless of external forcing [*Manabe and Wetherald*, 1975; *Wetherald and Manabe*, 1975; *Stone*, 1978]. This surprisingly simple relationship exhibited by the GCM is, however, due to the large changes in the transport of latent heat being canceled by changes in the transport of dry static energy. This cancelation is apparently subject to the equilibrium climate of the model (S. Manabe, private communication, 1980) and may not hold for drastically altered equilibrium states. Recent studies of an intermediate-sized model by *Held* [1978] seem to bear this out.

With the ranges obtained for $B = dI_0/dT_0$, $1.3 < B < 3.1$ W m^{-2} °C^{-1}, and for $Q \, dH_0/dT_0$, $0.2 < Q \, dH_0/dT_0 < 0.6$ W m^{-2} °C, we obtain a range 0.8°C $< \beta_0 < 3.4$°C. Although difficult to verify, this range probably brackets the actual sensitivity of the climate. It encompasses the sensitivities of most climate models—energy balance models (aside from those with the large albedo-temperature feedbacks), radiative-convective models [*Ramanathan and Coakley*, 1978], and general circulation climate models [*Lian and Cess*, 1977]. It is also consistent with the short-term response of the climate to increases in stratospheric aerosols as a result of volcanic eruptions [*Schneider and Mass*, 1975; *Mass and Schneider*, 1977; *Hansen et al.*,

1978]. It should be remembered, however, that the effect of at least one potentially significant feedback, cloud feedback, has not been included in the above estimates of β_0. As was mentioned before, what cloud cover changes will accompany climate changes and how they will influence the changes are subjects of current research.

5. SENSITIVITY TO CHANGES IN ORBITAL PARAMETERS

Over periods of 10^4–10^5 years the earth's orbit about the sun changes. *Milankovitch* [1941], among others, argued that these changes cause variations in the amount and distribution of solar radiation received by the earth, thereby influencing the climate. Milankovitch suggested that the orbital changes force the advance and retreat of glaciers. Indeed, evidence that the climate is so forced has been found in geological records. By examining sediments taken from deep ocean cores, *Hays et al.* [1976] have shown that the principal periods of climatic variation (100,000, 42,000, and 23,000 years) match those for changes in the eccentricity (105,000 years), the obliquity (41,000 years), and the longitude of perihelion (23,000 and 19,000 years). Many have used simple energy balance models in efforts to explain the glacial cycles as the result of orbital changes.

How energy balance models respond to orbital perturbations is understood through the effect of the perturbations on the forcing—the incident solar radiation. To start, we note that fractional changes in global average mean annual incident solar radiation are approximately given by $\frac{1}{2}\Delta e^2$ [*Berger*, 1978], where e is the eccentricity of the earth's orbit. Because the eccentricity has always been small ($e < 0.07$), the resulting changes in the solar constant have always been less than 0.2%. A 0.2% change in solar constant causes, according to the energy balance models, about a 0.4°C change in the global mean surface temperature. Such a change is an order of magnitude smaller than the changes that seem to have taken place [*Hays et al.*, 1976]. Owing to their insignificant magnitude, changes in energy balance models brought about by variations in the eccentricity will be neglected in the following discussion.

More important than changes in the mean annual solar radiation, however, are the variations in its latitudinal and seasonal distribution. These variations result from changes in the obliquity and longitude of perihelion. The seasonal variations are clearly represented by changes in the incident solar radiation for summer and winter caloric half years, as defined by *Milankovitch* [1941] [*Berger*, 1978]. We may derive these changes from the expression for $S(x, t)$,

$$S(x, t) = S_0(t) + S_1(t)P_1(x) + S_2(t)P_2(x) \qquad (70)$$

where to first order in e,

$$S_0(t) = 1 + 2e \cos(2\pi t - \Pi)$$

$$S_1(t) = S_1(\cos 2\pi t + 2e \sin \Pi \sin 2\pi t)$$

$$S_2(t) \simeq S_2[1 + 2e \cos(2\pi t - \Pi)]$$

Here $t = 0$ at the northern hemisphere's winter solstice, Π is the longitude of perihelion measured from the longitude of the winter solstice, and in the derivation of $S_2(t)$ we have neglected the first harmonic terms proportional to e that arise from the second harmonic, which results from the sun crossing the equator twice each year. The derivation of the terms in
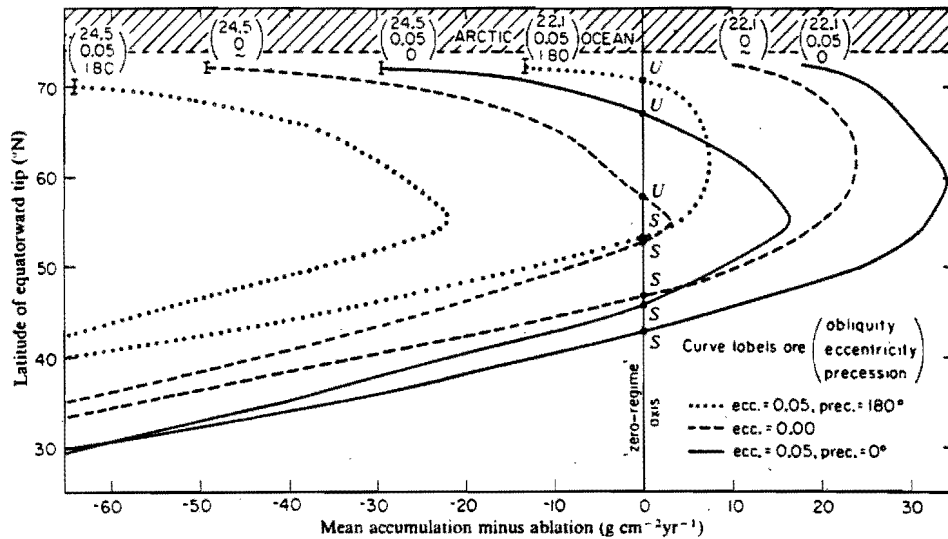
.Fig. 15. Stability of northern hemisphere ice sheet as a function of its latitudinal extent for various combinations of obliquity, eccentricity, and precession (longitude of perihelion measured from the position of the northern hemisphere winter solstice). To the right of the 'zero-regime' axis, mean accumulation exceeds ablation, and the ice sheet grows; to the left, ablation dominates, and the ice sheet shrinks. S denotes a stable equilibrium; U an unstable equilibrium [from *Pollard*, 1978].

(70) is outlined by *North and Coakley* [1979]. Averaging $S(x, t)$ over the summer and winter half years, we obtain

$$S_s = 1 - \frac{2}{\pi} S_1 P_1(x) + S_2 P_2(x) - \frac{4e}{\pi} \sin \Pi \, [1 + S_2 P_2(x)] \quad (71)$$

$$S_w = 1 + \frac{2}{\pi} S_1 P_1(x) + S_2 P_2(x) + \frac{4e}{\pi} \sin \Pi \, [1 + S_2 P_2(x)]$$

Changes in the incident radiation are thus given by

$$\Delta S_s = - \frac{2}{\pi} \Delta S_1 P_1(x) + \Delta S_2 P_2(x) - \frac{4}{\pi} \Delta(e \sin \Pi)[1 + S_2 P_2(x)]$$

$$(72)$$

$$\Delta S_w = \frac{2}{\pi} \Delta S_1 P_1(x) + \Delta S_2 P_2(x) + \frac{4}{\pi} \Delta(e \sin \Pi)[1 + S_2 P_2(x)]$$

The above expressions are the three-mode representations of the Milankovitch forcing as it has traditionally been calculated [*Milankovitch*, 1941; *Vernekar*, 1971; *Berger*, 1978].

From (72) we see that the change in the mean annual distribution of incident radiation is given by

$$\Delta S(x) = \tfrac{1}{2}(\Delta S_s + \Delta S_w) = \Delta S_2 P_2(x) \quad (73)$$

S_2 is easily shown to depend only on the obliquity δ_0. Because the range of obliquities remains small, $22.10° \leq \delta_0 \leq 24.51°$ [*Vernekar*, 1971], we may take $\Delta S_2 = 0.0115 \, \Delta\delta_0$, where $\Delta\delta_0$ is in degrees of arc.

Currently, $\delta_0 = 23.45°$, but 25,000 years ago, δ_0 was about 22.2°. This change in obliquity caused there to be less radiation incident at the poles and more incident at the equator. The change is thought to have spurred the glacial maximum 18,000 years ago. Inserting the altered distribution into a mean annual model, however, gives only a 1°–2° equatorward shift in the latitude of the ice line and a warming in low latitudes [*Budyko*, 1969; *Sellers*, 1970; *Saltzman and Vernekar*, 1971; *Coakley*, 1979]. These results clearly disagree with the ice line shift of approximately 15° and a cooling of several degrees at all latitudes deduced for the glacial maximum [*Climap Project Members*, 1976].

The small changes in the mean annual distribution of incident radiation and the disappointingly small response of mean annual models have led some to suggest that seasonal variations need to be considered when estimating the effect of Milankovitch forcing. Obviously, (72) indicates that variations for each season will be larger than those for the annual mean. Results of seasonal models that allow for these variations, however, fail to differ significantly from those of the mean annual models [*Suarez and Held*, 1976, 1979; *North and Coakley*, 1979]. S_1, to first order in e, is easily shown to depend only on δ_0, and thus, like S_2, we find $\Delta S_1 = -0.016 \, \Delta\delta_0$. Because S_1 contributes only a small increment to T_0 and T_2, ΔS_1 raises the response of a seasonal model only slightly over that of a mean annual model. Likewise, by considering as in section 3 the mean annual residuals contributed by the terms proportional to e in (72) we find that for the last 25,000 years these terms contribute, at most, variations of the order of 0.1°C in T_0 and T_2. Also, if we allow for differences between the annual mean temperatures of the two hemispheres, the terms that couple the seasonal variation of albedo with changes in the longitude of perihelion contribute, at most, 0.2°C to the annual mean component of T_1. Thus neither mean annual nor seasonal models give responses that would support the Milankovitch theory.

Of course, as was mentioned in the two previous sections, simplicity and questionable parameterizations may be the reason that energy balance models fail to give large responses. Perhaps if more physical processes were modeled, more feedbacks included, and more realism added, the models would become more sensitive.

Some additional features have been added recently. *Pollard* [1978] added Weertman's glacier model [*Weertman*, 1976] to a simple three-mode seasonal model. Because it allows for the ablation of snow and ice by incident solar radiation, the glacier model contributes far more to the sensitivity of the seasonal model than to that of the mean annual model. The enhanced sensitivity is indicated by the sensitivity of the model to changes in perihelion as shown in Figure 15. Nevertheless, if we scale the results shown in Figure 15, we find that the

model, even with enhanced sensitivity, would predict only a 4°–5° shift in the ice line for the obliquity change connected with the 18,000 years B.P. glacial maximum. The addition of a glacier model by itself has so far proven insufficient to obtain the desired results.

Another factor to consider is the zonal asymmetry of ice age climates. Most of the models mentioned so far have been zonally symmetric. Reconstructions of the last glacial maximum indicate, however, that in the northern hemisphere, ice extended much further equatorward over continents than over oceans [*Climap Project Members*, 1976]. *Hartmann and Short* [1979] have argued that the glacial maximum and its evident asymmetry may have been the response to a zonally asymmetric wave in the surface temperature. Using an energy balance model that contains a prescribed asymmetry in the surface temperature, they obtain an ice-age-like response when they insert reasonable amplitudes for the asymmetric term. With this additional component, however, the model appears to be no more sensitive to changes in the incident radiation. In Figure 16 the global mean temperature is plotted as a function of solar constant for different amplitudes of the zonally asymmetric component. The nearly identical slopes of the curves indicate a common sensitivity. From this result we expect that allowing for the asymmetry would not greatly enhance the sensitivity of the model to orbital changes. In fact, by allowing temperatures over continents to differ from those over oceans, *Suarez and Held* [1976, 1979] incorporated a degree of asymmetry into their model. The results of their model, however, are not significantly different from those of zonally symmetric models.

Still, failures to support the Milankovitch theory may only reflect the inadequacies of the models. Most models that have been used to test the theory have included only one feedback that could amplify the response—the albedo-temperature feedback. Experience with these models, however, leads us to search for additional feedbacks that either by themselves or working together could amplify the response [*Cess and Wronka*, 1979; *Cess*, 1978]. An especially new and interesting approach involves coupling various nonlinear components of the internal climate system in such a way that self oscillations can occur. In some cases, ice age time scales have been generated [cf. *Källén et al.*, 1979; *Ghil*, 1981].

6. STABILITY THEORY

When a model, such as the models discussed in section 2, has been solved and several solutions found for the same external conditions, we should study the stability of each solu-
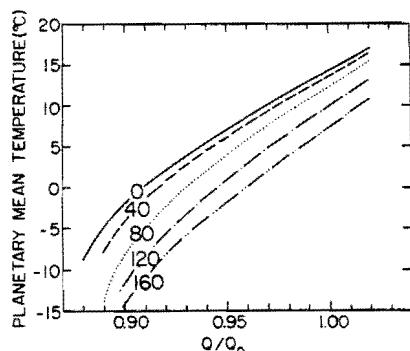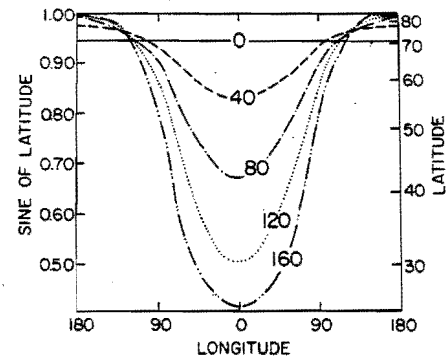

Fig. 16b. Sine of the latitude of the $-10°C$ isotherm as a function of longitude for the five values of asymmetric forcing [from *Hartmann and Short*, 1979].

tion. *Schneider and Gal-Chen* [1973] were the first to study the effect of various perturbations on a Sellers-type model at fixed solar constant. They found that the present climate was stable but that if a large enough cold perturbation ($\sim20°C$) was applied at all latitudes, the solution failed to return to the present climate but instead plunged to the ice-covered earth solution. Subsequently, linear stability results were obtained for the Budyko model by *Held and Suarez* [1974] and *Su and Hsieh* [1976]; other analyses for diffusive models were performed by *North* [1975a], *Ghil* [1976], *Frederiksen* [1976], and *Drazin and Griffel* [1977]. The most general linear stability analysis for a wide class of models was performed by *Cahalan and North* [1979]. An approach for a finite amplitude stability analysis was suggested by *Ghil* [1976], and a complete study along the same lines based upon a variational principle was given by *North et al.* [1979]. Incorporating ideas taken from all of the above mentioned studies, we shall now discuss the stability of the model solutions.

In performing a stability analysis we study the time-dependent response of the model to perturbations from its equilibrium state. We shall restrict the discussion here to mean annual models. A climatic state not in equilibrium must have a heat storage term added to the energy balance equation, C $\partial T(x, t)/\partial t$, where C is the heat capacity per unit area for a column of the earth-atmosphere system. As was mentioned in section 3, the vast difference in C over land and ocean leads to some error associated with simply taking a zonally averaged C, but we shall ignore this complication in the present section. It is easily seen that C merely scales the time in our present discussion, and since we are only asking whether or not a given solution is stable, regardless of time scale, we may set C equal to unity.

Linear Stability of Global Models

To illustrate the concept of stability, consider a model with no ice cap feedback. Its time behavior may be studied by adding the storage term to (8):

$$(\partial T_0(t)/\partial t) + A + BT_0(t) = Q(1 - \alpha_p) = QH_0 \quad (74)$$

It is easily shown that any deviation from the equilibrium solution given by (8) decays back to equilibrium exponentially with a time constant equal to $1/B$ (times the heat capacity per unit area, C, which we have set to unity). The outgoing radiation therefore damps the solution back to equilibrium. For a column of atmosphere only, this relaxation time is about 58 days. Larger values of B (increased negative feedback) lead to

Fig. 16a. Global average temperature as a function of solar constant for five values of zonally asymmetric forcing (watts per square meter).
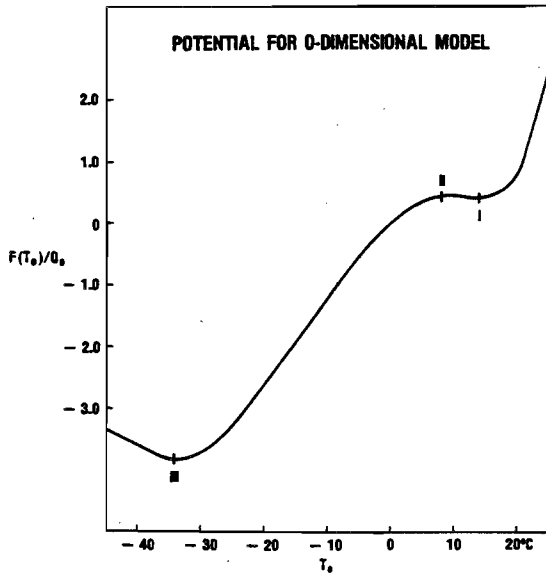
Fig. 17. Potential function for the finite amplitude stability analysis of the zero-dimensional climate model defined by (8), (13), (75), and (82). The extrema are labeled as in Figures 1 and 2.

increased damping. With no albedo feedback the model is linear, and it has only one solution that is always stable.

The next model of interest allows some temperature dependence in the planetary albedo; it is the zero-dimensional ice cap model discussed earlier (cf. (13)). In this case,

$$(\partial T_0(t)/\partial t) + A + BT_0(t) = QH_0[x_s(T_0)] \qquad (75)$$

and the model may be linearized for small deviations from a steady state solution, say, T_0^0. Then if we let

$$T_0(t) = T_0^0 + \delta T(t) \qquad (76)$$

we may write

$$\delta\dot{T}(t) + B\delta T(t) = Q(dH_0/dT_0)\delta T(t) \qquad (77)$$

where we have made use of the steady state condition given by

$$A + BT_0^0 = QH_0(T_0^0) \qquad (78)$$

Taking a derivative along the curve given by (78), we obtain

$$\frac{B\,dT_0^0}{dQ} = H_0 + \left(\frac{Q\,dH_0}{dT_0^0}\right)\frac{dT_0^0}{dQ} \qquad (79)$$

which in turn may be used to simplify (77), giving

$$\delta\dot{T}(t) + H_0\left(\frac{dT_0^0}{dQ}\right)^{-1}\delta T(t) = 0 \qquad (80)$$

Equation (80) establishes a theorem which may be generalized to a very large class of climate models: If the steady state solution is on a branch with dT_0/dQ positive, the solution will be stable; if this is not so, the positive albedo-temperature feedback $Q\,dH_0/dT_0$ is larger than the IR radiative damping B, and the solution will be unstable. To summarize for the simplified global model:

$$\begin{aligned} dT_0/dQ > 0 &\Leftrightarrow \text{stability} \\ dT_0/dQ < 0 &\Leftrightarrow \text{instability} \end{aligned} \qquad (81)$$

Potential Function for Global Models

It is also fairly easy to examine qualitatively the response of the simplified global model to large (nonlinear) perturbations. We present the analysis here, as it will prove useful in the more complicated examples to follow. Our method will be to construct a potential function (sometimes called the Lyapunov function [cf. *North et al.*, 1979]) that will completely describe the model and its behavior away from steady state. Consider the function

$$F(T_0) = AT_0 + \tfrac{1}{2}BT_0^2 - QJ_0(T_0) \qquad (82)$$

where

$$J(T_0) \equiv \int_0^{T_0} H_0(T_0')\,dT_0' \qquad (83)$$

is determined from the temperature-dependent co-albedo shown in Figure 1. A graph of the potential $F(T_0)$ is shown in Figure 17. Note that the extrema of F (points where $dF/dT_0 = 0$) are given by the energy balance equation (78); therefore these extrema correspond to the roots I, II, and III of Figure 1. Note also that in terms of $F(T_0)$, (75) becomes

$$\dot{T}_0 = -dF/dT_0 \qquad (84)$$

Furthermore,

$$dF/dt = (dF/dT_0)\dot{T}_0 = -(\dot{T}_0)^2 \leq 0 \qquad (85)$$

Thus the time derivative of T_0 is proportional to the slope of F at T_0, and F always decreases with time. The implication is that the shallow local minimum I (the present climate) is stable, the maximum II is unstable, and the ice-covered planet III is stable. Figure 17 makes it entirely plausible that a uniform $-20°C$ perturbation applied to the latitude-dependent models would probably take the solution 'over the hill' and into the ice-covered planet valley, as was discovered numerically by *Schneider and Gal-Chen* [1973].

Note that the 'slope-stability' theorem (81) and the existence and qualitative form of a potential function (82) are independent of the exact parameterizations used for the albedo and IR radiative flux. As was noted in sections 2, 3, and 4, much remains to be done in the area of parameterization theory, so that results independent of details or numerical values of constants are of special interest. In the remainder of this section we will illustrate how the slope-stability theorem and the potential function may be generalized to the class of one-dimensional models. We begin with the linear stability analysis.

Linear Stability of One-Dimensional Models

The time-dependent energy balance equation is given by

$$\frac{\partial I(x, t)}{\partial t} - \frac{\partial}{\partial x} D(x)(1 - x^2)\frac{\partial}{\partial x} I(x, t) + I(x, t) = QS(x)a(x, x_s) \qquad (86)$$

and the ice line condition by

$$I(x_s, t) = I_s \qquad (87)$$

In these equations we have used $I = A + BT$ rather than T as the dependent variable. The time in $\partial I/\partial t$ has been scaled by C/B, where C is the heat capacity per unit area. Expanding I in terms of the eigenfunctions of the diffusion operator, $f_n(x)$,

we may use the orthogonality condition (47) to determine the coefficients. From (86) we obtain

$$I_n + l_n I_n = Q h_n(x_s) \qquad (88)$$

where we have defined expansion coefficients for I,

$$I_n(t) = \int_0^1 f_n(x) I(x, t) \, dx \qquad (89)$$

and for the solar heating,

$$h_n(x_s) = \int_0^1 f_n(x) S(x) a(x, x_s) \, dx \qquad (90)$$

and $l_n = \mu_n + 1 \geq 1$.

To linearize about the present climate, let

$$I_n(t) = I_n^0 + \delta I_n(t) \qquad (91)$$

and

$$x_s(t) = x_0 + \delta x_0(t) \qquad (92)$$

with the steady state given by

$$l_n I_n^0 = Q h_n(x_0) \qquad (93)$$

and the ice line condition by

$$\sum_n I_n^0 f_n(x_0) = I_s \qquad (94)$$

These latter equations define the equilibrium state denoted by (x_0, I_n^0) whose stability is to be tested. Linearizing (88), we obtain

$$\delta \dot{I}_n + l_n \delta I_n = Q h_n'(x_0) \, \delta x_0 \qquad (95)$$

The perturbed ice line δx_0 can be related to the δI_n through (94):

$$\delta x_0 = - \left(\sum_l f_l \, \delta I_l \right) \left(\sum_m f_m' I_m^0 \right)^{-1} \qquad (96)$$

In (96) and in what follows we suppress the argument x_0 in f_m, f_n', h_n, and h_n'. Substituting (96) in (95) leads to an infinite set of simultaneous, homogeneous, linear, first-order differential equations for the $\delta I_n(t)$. By substituting $\delta I_n(t) = \delta I_n e^{-\lambda t}$ we may find the set of values of λ for which the equations are satisfied. This turns out to be the eigenvalue problem

$$\sum_m M_{nm} \delta I_m = \lambda \delta I_n \qquad (97)$$

where

$$M_{nm} = l_n \delta_{nm} + \gamma f_n f_m \qquad (98)$$

$$\gamma = Q \Delta a S(x_0) \left(\sum_m I_m^0 f_m' \right)^{-1} \qquad (99a)$$

To obtain (99a), we assumed the albedo to be a step function in x. For this case the integral (90) can be differentiated, giving a delta function under the integral sign leading to the result

$$h_n' = \Delta a S(x_0) f_n \qquad (99b)$$

where $\Delta a > 0$ is the discontinuity in $a(x, x_s)$ at $x = x_s$.

The stability of the system with steady state (x_0, I_n^0) is de-termined by the sign of the eigenvalues λ. Because M_{nm} is real and symmetric, all eigenvalues are real and bounded from below. If the lowest eigenvalue is negative, the system is unstable; δI grows exponentially with time. If the lowest ei-genvalue is positive, the solution is stable; δI decays ex-ponentially with time. By casting the eigenvalue problem into a different form we can determine the sign of the lowest root.

To determine the sign, we rearrange (97) and use (98) to ob-tain

$$(l_n - \lambda) \delta I_n = -\gamma f_n \sum_m f_m \delta I_m \qquad (100)$$

Dividing this expression by $l_n - \lambda$, multiplying by f_n, and sum-ming over n, we obtain

$$1 = -\gamma \sum_n \left(\frac{f_n^2}{l_n - \lambda} \right) \qquad (101)$$

This relation is a transcendental equation that is satisfied for certain discrete values of λ, the stability eigenvalues. By fur-ther rearrangement we arrive at the sign of the lowest eigen-value. With (99a), (101) becomes

$$\sum_n \left(\frac{f_n^2}{l_n - \lambda} + \frac{I_n^0 f_n'}{Q b S(x_0)} \right) = 0$$

which with (93) becomes

$$\sum_n \left(\frac{b S(x_0) f_n^2}{l_n - \lambda} + \frac{h_n f_n'}{l_n} \right) = 0 \qquad (102)$$

Since

$$\frac{d}{dx_0} I_s = 0 = \frac{d}{dx_0} \left[Q \sum_n \frac{h_n f_n}{l_n} \right]$$

$$\sum_n \frac{h_n f_n'}{l_n} = -\frac{1}{Q} \frac{dQ}{dx_0} I_s - \sum_n \frac{h_n' f_n}{l_n} \qquad (103)$$

Substituting (103) and (99b) into (102), we obtain

$$\frac{dQ}{dx_0} = \lambda \frac{Q^2}{I_s} \sum_n \frac{b S(x_0) f_n^2}{l_n (l_n - \lambda)} \qquad (104)$$

As a function of λ the right-hand side of (104) has a zero at $\lambda = 0$ and a sequence of poles with positive residue at the points $\lambda = l_n$ ($l_n > 1$). This is sufficient for us to make the schematic plot shown in Figure 18. If the horizontal line corresponding to the constant dQ/dx_0 is also plotted on the graph, the roots $\lambda^{(i)}$ are at the intersections of these curves. Clearly, if dQ/dx_0 is positive, all roots are positive, and the solution is stable. If dQ/dx_0 is negative, the lowest root becomes negative, and the solution becomes unstable. These results constitute the slope-stability theorem for the simple one-dimensional models.

The proof sketched above can be generalized and made rig-orous for all models that have positive Green's functions (cf. (49)) [Cahalan and North, 1979]. Note that the slope-stability theorem holds only for north-south symmetric solutions and for models with ice caps that follow isotherms; that is, the co-albedo may be written as $a(x, x_s)$. Models possessing an al-bedo with the functional form $a(T)$ may have solutions that are unsymmetrical [Drazin and Griffel, 1977]; in such cases the proof of the theorem fails. The proof of the theorem requires the existence of the single index x_0 that picks out which of the several solutions one is examining for a given Q.
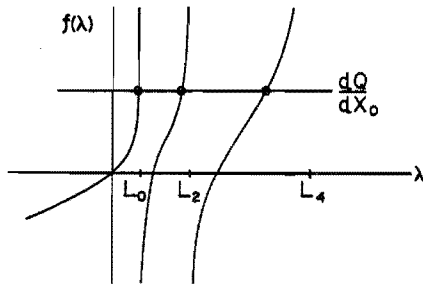
Fig. 18. Schematic graph of the right-hand side of (105) (denoted by $f(\lambda)$ in the figure) versus the stability parameter λ. Intersections with the (flat) dQ/dx_0 graph indicate discrete eigenvalues $\lambda^{(j)}$ of the system. Note that if dQ/dx_0 is negative, the lowest eigenvalue must be negative, implying instability.

It should be noted that the slope-stability theorem for the one-dimensional models differs slightly from that for the global model (81). The sign of dT_0/dQ and dx_0/dQ may differ near a cusp at which $dx_0/dQ = 0$. To see how this may happen, we differentiate (93) for $n = 0$, $A + BT_0 = Qh_0$, to obtain

$$\frac{B \, dT_0}{dQ} = h_0 + Q \, \frac{dh_0}{dx_0} \, \frac{dx_0}{dQ} \tag{105}$$

Both h_0 and dh_0/dx_0 are positive. Therefore dT_0/dQ remains positive near a cusp where dx_0/dQ is small and negative. In that case the solution is unstable even though β_0 is positive. On the other hand, near a bifurcation the magnitudes of dx_0/dQ and dT_0/dQ are large and of the same sign. So the positivity of β_0 is always necessary for stability, and if we exclude cusps, then it is sufficient as well.

Potential Functional for One-Dimensional Models

We consider now the finite amplitude stability analysis of the one-dimensional $a(T)$ models. Our aim is to construct a potential function analogous to (83). In the zero-dimensional case the potential (Lyapunov function) $F(T_0)$ was a function of only one variable; its local extrema gave the steady state solutions to the energy balance equation. If the solution was perturbed, T_0 changed in time according to the negative slope of $F(T_0)$, which itself continually decreased in time until a (steady state) extremum was reached. Clearly, a local minimum corresponded to a stable solution, while a local maximum corresponded to an unstable solution.

The analogous procedure for one-dimensional models is more complicated. The potential must be a function of $T(x)$ at each local point x. That is, it must be a functional $F[T]$. The nature of this kind of mathematical object is most easily described by example. We shall therefore present a functional and show that it has the desired properties [North et al., 1979]; a similar method was suggested by Ghil [1976]. We take the functional to be given by

$$F[T] = \int dx \left[\tfrac{1}{2} D(1 - x^2)T_x^2 + R(T) - QS(x)C(T) \right] \tag{106}$$

where $T_x = dT/dx$,

$$R(T) = \int^T I(T') \, dT' \tag{107}$$

and

$$C(T) = \int^T a(T') \, dT' \tag{108}$$

It is relatively straightforward [North et al., 1979] to show that if δF is to vanish (local extremum) for an arbitrary variation

$\delta T(x)$ in the temperature field, the corresponding energy balance equation must be satisfied (steady state solution). North et al. [1979] also show that these solutions are stable if the extremum is a local minimum and unstable if the extremum is either a saddle point or a local maximum.

Here we shall illustrate the procedure for the model just used to prove the slope-stability theorem. The co-albedo, however, will be given by

$$a(I) = a_0\theta(I - I_s) + a_1\theta(I_s - I) \tag{109}$$

where $\theta(Z)$ is the unit step function, $\theta = 0$ for $Z < 0$, and $\theta = 1$ for $Z \geq 0$. Note that the step function albedo (109) is the one case where models having the co-albedo functional dependence $a(T)$ and models having the functional dependence $a(x, x_s)$ are identical. It is easier to visualize the functional $F[A + BT] = F[I]$ in spectral form, $I = \sum_n I_n f_n(x)$. In spectral form, F may be thought of as a function of the variables $I_0, I_2, I_4, \cdots$, where for symmetric models we use only even indices. An extremum of $F(I_0, I_2, \cdots)$ may be expressed as $\partial F/\partial I_n = 0$ for all n.

Substituting (109) into (106) and using the orthogonality condition (47) for the f_n, we obtain

$$F(I_0, I_2, \cdots) = \sum_n \tfrac{1}{2} l_n I_n^2 - M(I_0, I_2, \cdots) \tag{110}$$

where

$$M(I_0, I_2, \cdots) = Q \int_{-1}^{1} S(x)(I - I_s)[a_0\theta(I - I_s) + a_1\theta(I_s - I)] \, dx \tag{111}$$

It is understood that $\sum_n f_n(x)I_n$ is to be substituted for I in (111). The condition that the $\partial F/\partial I_n$ vanish simultaneously leads to

$$l_n I_n = Q \int S(x) f_n(x)[a_0\theta(I - I_s) + a_1\theta(I_s - I)] \, dx \tag{112}$$

$$l_n I_n = Q h_n(x_s) \tag{113}$$

where we have used (29). Note that (113) represents the decomposition of the energy balance equation (27).

In the neighborhood of an extremum, let the radiation field corresponding to a particular extremum (steady state) be given by $I^{(0)}(x)$ or, equivalently, by $I_0^{(0)}, I_2^{(0)}, \cdots$. Near by (in function space) we may write $I(x) = I^{(0)}(x) + \phi(x)$, or the de-
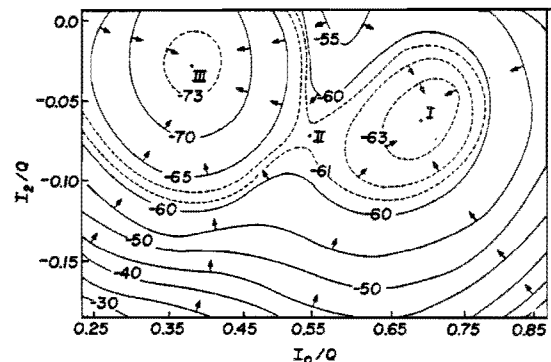

Fig. 19. Contours of the potential function (111) for a two-mode one-dimensional climate model plotted in the I_0, I_2 plane, the two-mode amplitudes. The states I, II, and III correspond to notation in the previous figures [from North et al., 1979].

viation may be written in terms of its spectral components ϕ_0, ϕ_2, $\cdots$. Expanding $F[I]$ about the local extremum, we obtain

$$F(I_0, I_2, \cdots) \cong F_0 + \sum_n \left[\frac{\partial F}{\partial I_n}\right]_0 \phi_n + \frac{1}{2} \sum_{n,m} \left[\frac{\partial^2 F}{\partial I_n \partial I_m}\right]_0 \phi_n\phi_m + \cdots \tag{114}$$

where the subscript zero denotes evaluation at the extremum. The terms linear in ϕ_n vanish because $\partial F/\partial I_n$ vanishes at the extremum. Up to the terms considered, F is locally a quadratic in ϕ_n. The matrix elements

$$N_{nm} = (\partial^2 F/\partial I_n \partial I_m)_0 \tag{115}$$

are the structure constants for the geometrical surface, $F(I_0, I_2, \cdots)$. If all eigenvalues of N_{nm} are positive, the surface is concave upward; if one or more of the eigenvalues are negative, the surface is locally a saddle point. We proceed to show that these eigenvalues are the stability eigenvalues studied earlier.

First note that if the temperature field is allowed to be a function of time, then by following the approach for the zero-dimensional models we have

$$\dot{I}_n = -(\partial F/\partial I_n)(I_0, I_2, \cdots) \tag{116}$$

that is, the time derivative is given by the gradient in this multidimensional space. For infinitesimal departures from steady state we set $[I_n(t) = I_n{}^0 + \phi_n e^{-\lambda t}]$ in (116), expand about $\phi_n = 0$, and obtain

$$-\lambda\phi_n = -\sum_m \left[\frac{\partial^2 F}{\partial I_n \partial I_m}\right]_0 \phi_m \tag{117}$$

$$-\lambda\phi_n = -\sum_m N_{nm}\phi_m \tag{118}$$

The latter equation concludes the proof that the local geometrical structure constants of $F(I_0, I_2, \cdots)$ at a steady state solution yield the stability eigenvalues for that particular steady state. Equation (118) is the analog of the simple equation (80) or, in the one-dimensional case, equation (97).

Finally, as a conclusion to this section, consider the time behavior of the value of $F(I_0, I_2, \cdots)$ when the point $(I_0, I_2, \cdots)$ is governed by the time-dependent equation (89):

$$\frac{dF}{dt} = \sum_n \frac{\partial F}{\partial I_n} \dot{I}_n \tag{119}$$

$$\frac{dF}{dt} = -\sum_n (\dot{I}_n)^2 \tag{120}$$

where we have used (116). This latter result is the multidimensional analog of (85). It has a corresponding interpretation: initial departures of the state $(I_0, I_2, \cdots)$ from a local extremum of F lead to a trajectory of the point such that F decreases. The point will continue down the gradient of F until a local extremum is found. Clearly, local maxima and saddle points are unstable.

It was shown in section 2 that a two-mode truncation of the spectral representation gives a good approximation in many cases. In this case we can actually plot a contour map of F in the I_0, I_2 plane. This is shown in Figure 19; the example is for constant diffusion so that $f_n(x) \propto P_n(x)$. Note that the scales of I_0 and I_2 are different in the text, since the $P_n(x)$ are not orthonormal. This two-dimensional map is to be compared with its one-dimensional analog (zero-dimensional model) in Figure 17. The labels I, II, and III correspond to the analogous labeling of earlier figures. Physical interpretation of the figure follows directly from the previous discussion.

Before leaving this subject we note that the Lyapunov functional $F[T]$ gives rise to a variational principle for the Budyko-Sellers climate models. Although the functional developed here was strictly a mathematical construction, it is tempting to speculate that there is an underlying physical principle analogous to extremum conditions in thermodynamics. If $F[T]$ can be related to the rate at which entropy is dissipated in the system, then the extremum principle would be in line with Prigogine's theory of nonequilibrium thermodynamic states [*Prigogine*, 1968]. *Golitsyn and Mokhov* [1978] have shown that the linear climate models (no ice-albedo feedback) can be formulated so that they satisfy Prigogine's condition. Unfortunately, such models have but one stable solution and therefore fail to test the general applicability of the extremum condition. *Paltridge* [1975, 1978] has suggested on the basis of energy budget observations that the climate system is governed by a somewhat different, but equally simple, extremum principle. Whether the behavior of such a complex system can be so simply characterized is a tantalizing but open question.

7. STATIONARY PERTURBATION THEORY

The sensitivity of climate models to stationary perturbations has received considerable attention. Many recent papers have offered estimates of the change in surface temperature caused by changes in the concentrations of various radiatively active trace gases in the atmosphere, by changes in the surface albedo as a result of man's activities, by changes in the aerosol content of the atmosphere, by additions of waste heat from energy consumption, and by many other changes. In this section we shall derive a formula for the infinitesimal change in climate as the result of small perturbations added to the energy balance equation. The formula has little practical utility; nevertheless, it offers insight into the qualitative response of a large class of models. For simplicity we shall study perturbations which are sufficiently small that linear approximations can be applied. Analytic solutions to nonlinear systems with large perturbations have been obtained by Salmún [*Salmún*, 1979; *Salmún et al.*, 1980].

Consider the class of energy balance models discussed in section 2. There we derived a Green's function G_0, given in (48), that describes the response to a ring of heat added at a given latitude, the ice line being held fixed. If G_0 is known, the ice line latitude is determined for any Q through (50). In turn, the temperature field given by (49) is completely determined. Now we shall hold $Q = Q_0$ fixed and add an amount of heat g with some given latitudinal distribution $u(x)$ (hemispherically symmetric, positive, and normalized to unit integral). To add this heat, (39) is replaced by

$$L[T_g] + A(x) = Q_0 S(x)a(x, x_s) + gu(x) \tag{121}$$

and the integral equation analogous to (49) becomes

$$T_g(x) = \int_0^1 dy\, G_0(x, y)[Q_0 S(y)a(y, x_s) - A(y) + gu(y)] \tag{122}$$

Setting $T_g(x_s) = T_s$ in (122) gives an expression which determines the ice line latitude for a given g. By equating this expression to the previous T_s expression, (49) evaluated at $x = x_s$, we find that the terms involving A cancel, giving

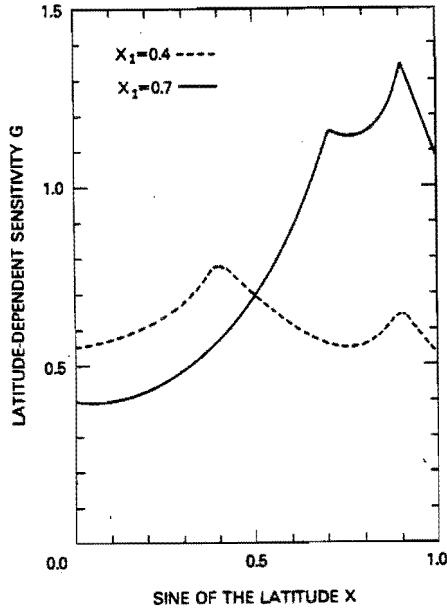$$(Sa)_s Q(x_s) = (Sa)_s Q_0 + (u)_s g(x_s) \tag{123}$$

where

Fig. 20. Latitude-dependent sensitivity (i.e., stationary response function) $G(x, x_1)$ computed with diffusive transport, Budyko's infrared rule, and an isothermal ice cap edge at $x_0 = 0.9$. The two cases shown are for perturbations at 23.5° latitude ($x_1 = 0.4$) and at 45° latitude ($x_1 = 0.7$). In both cases, additional heat is absorbed in the ice edge region, and the effect increases with the global temperature sensitivity (here $\beta_0 = 1.6°C$ per 1% change in solar constant) as well as with the proximity of the perturbation to the ice edge.

$$(Sa)_s = \int_0^1 dy \, G_0(x_s, y)S(y)a(y, x_s) \qquad (124)$$

and

$$(u)_s = \int_0^1 dy \, G_0(x_s, y)u(y) \qquad (125)$$

This result allows us to determine $x_s(Q_0, g)$ from the unperturbed result $x_s(Q, 0)$.

We now assume that g is small, so that the temperature field will be nearly equal to the $g = 0$ value. That is,

$$T_g = T_0 + \delta T \qquad (126)$$

where T_0 is given by (49) with $Q = Q_0$ and δT is small. Correspondingly, the ice line latitude is given by

$$x_s = x_0 + \delta x_s \qquad (127)$$

where x_0 is the unperturbed ice line and δx_s is small. By expanding $a(y, x_s)$ in (122) and $Q(x_s)$ in (123) to first order in δx_s we may eliminate T_0 and Q_0 to obtain

$$\delta T(x) = \int_0^1 dy \, G_0(x, y) \left[Q_0 S(y) \frac{\partial a}{\partial x_0} (y, x_0)\delta x_s + gu(y) \right]$$
$$+ O(\delta x_s^2) \qquad (128)$$

and

$$\delta x_s = \frac{dx_0}{dQ} \frac{(u)_0}{(Sa)_0} g + O(g^2) \qquad (129)$$

According to (129) the shift in the ice line for a given g is directly proportional to the ice edge sensitivity dx_0/dQ. By substituting this shift into (128) we obtain the final result

$$\delta T(x) = g \int_0^1 dz \, G(x, z)u(z) + O(g^2) \qquad (130)$$

where

$$G(x, z) \equiv G_0(x, z)$$

$$+ \frac{dx_0}{dQ} \frac{Q_0}{(Sa)_0} \left[\int_0^1 dy \, G_0(x, y)S(y) \frac{\partial a}{\partial x_0} (y, x_0) \right] G_0(x_0, z) \qquad (131)$$

Setting $u(z) = \delta(z - z_0)$ in (130) shows that $G(x, z_0)$ represents the temperature response to a ring of heat added at a given latitude. The response includes to first order the effect of the ice line shift. Since the problem has been linearized, the response to an arbitrary distribution is given by the appropriate superposition of localized sources, as is indicated by (130).

We should recognize that the first term in (131) is the response when there is no ice-albedo feedback. The second term is the response due to the albedo feedback. Note that the feedback term is multiplied by dx_0/dQ, the slope of the ice line solar constant curve. Thus for small perturbations the slope of the ice line curve governs the thermal response of a climate model to any perturbation. As a result the fundamental sensitivity $\beta_0 = (Q/100) \, dT_0/dQ$ of a model is an indicator of its sensitivity to any perturbation.

For the step function albedo, β_0 and dx_0/dQ may be related by differentiating (31):

$$\beta_0 = \frac{1}{100B} \left[A + BT_0 + Q^2 S(x_0)\Delta a \frac{dx_0}{dQ} \right] \qquad (132)$$

where Δa is the change in albedo at $x = x_s$. (This is a particular case of (105).) As a numerical example, consider the case of a step function albedo for which the expression for G simplifies to

$$G(x, x_1) = G_0(x, x_1) + \frac{\beta_0 - 1.12°C}{0.42°C} G_0(x, x_0)G_0(x_0, x_1) \qquad (133)$$

where (132) has been used. (Recall from (9) that $1.12°C$ is the sensitivity when the albedo remains constant.) Since $G_0(x, x_1)$ peaks at $x = x_1$ (see Figure 7, for example), the feedback term tends to increase the response near the ice line, $x \simeq x_0$, and this effect is largest when the added heat is closest to the ice line, $x_1 \simeq x_0$. Figure 20 illustrates these features for a tropical source ($x_1 = 0.4$) and a mid-latitude source ($x_1 = 0.7$), where we have used the diffusive G_0, $\beta_0 = 1.6°C$, and $x_0 = 0.9$. For a source which is broadly distributed, only the peak at the ice edge appears. This kind of effect has also been observed in detailed models having many feedbacks [*Manabe and Wetherald*, 1975].

Plots of $g(x_s)$ show that the range of g for which the linear approximation is valid tends to be smaller when heat is added closer to x_0. This range also depends upon the $Q(x_s)$ curve characteristics [*Salmun*, 1979; *Salmun et al.*, 1980]. For a range of large negative g the slope dx_s/dg usually changes sign, and it can be shown by arguments analogous to those in section 6 that a negative slope is necessary and sufficient for instability.

8. FLUCTUATIONS

In previous sections we have focused on quasi-periodic changes associated with seasonal and orbital effects. However, typical climatic time series also exhibit large amounts of nonperiodic variability. In this section we shall extend the models considered so far by including this broad distribution of variance having periods that range from seasons to centuries. The

low-frequency part of this range, say, periods from decades to centuries, is particularly difficult to observe because instrumental records tend to be too short and proxy records are difficult to interpret. Nevertheless, such low-frequency natural variability may contain information on the true sensitivity of the climate. That is, the effects of possible future perturbations of the climate due to various external causes may be estimated from past responses to natural fluctuations associated with internal degrees of freedom. In sections 2 and 6 the stability of a given steady state was related to the sensitivity. One of the goals in this section is to show how the natural variability may be related to the sensitivity. Such a relationship was suggested by *Leith* [1975, 1978] and is known in statistical mechanics as the 'fluctuation-dissipation theorem.'

In long-term climatic records, slower fluctuations generally have larger amplitudes. This feature is also a characteristic of Brownian motion, the random movement of small particles suspended in a liquid. Over short time periods, only a few molecules collide with a given particle, and its displacement from its original location is small, but over long periods there is some chance that many collisions drive the particle far from its original position. The fluid has two components: the molecules, which move and change direction rapidly, and the particles, which move slowly. A similar scale separation is expected to exist between the relatively rapid evolution of synoptic weather systems and the more sluggish climatic components such as the global average temperature and the pole-to-equator temperature gradient.

The suggestion that broadband climatic fluctuations may be a cumulative effect due to variations on much shorter time scales was made by *Mitchell* [1966] in connection with sea surface temperature anomalies. The two-time-scale approximation was given a general formulation by *Hasselmann* [1976], who emphasized the role of negative feedback processes in limiting climatic variability. This approach was applied to simple ocean models by *Frankignoul and Hasselmann* [1977] and *Frankignoul and Müller* [1979], to Budyko's energy balance model by *Lemke* [1977], and to a global energy balance model by *Fraedrich* [1978]. *Robock* [1978] has performed numerical computations of effects of fluctuations in energy balance models.

Preliminaries

We shall think of the complete time history of the global average temperature, for example, as a single 'realization' of a random phenomenon. If we imagine an infinite population of essentially identical planets in the same orbit around the sun, the collection or 'ensemble' of all the time series of global temperatures constitutes a 'stochastic process,' generally defined as any ordered (by time in this case) set of random variables [*Jenkins and Watts*, 1968]. The probability that the temperature is in a given range may be estimated from a sample of the population by determining the fraction of planets within the sample having temperatures in that range. Such a result generally depends on when the count is taken, particularly if there are changes in external forcing. We shall assume that such dependence may be removed by subtracting the effects of external forcing. In our example of an ensemble of planets this might be done by considering only the deviations from a time-dependent ensemble average temperature. The associated stochastic process is said to be 'stationary.'

Since no such ensemble of planets is available, we are forced to try to determine the statistics of any stochastic component of the climate from a single realization. This might be possible if the values of climatic quantities at a given time are uncorrelated with the values at a much later time, so that the complete record may be treated as an ensemble of independent records. We shall assume that this is the case and that any quantity determined by time averaging over a sufficient length of a single record will equal its corresponding ensemble average value. The stationary stochastic process is then said to be 'ergodic.'

A general stochastic process, then, is an ensemble of functions that depend on time. Each function represents a point in a 'sample space' of possible experimental outcomes (different planets in the above example), which we may label by the parameter ϵ. We use the notation $T_0(t, \epsilon)$ to represent a different function of time for each value of ϵ. Note that $T_0(t, \epsilon)$ is also a random variable in ϵ at any given time. We shall use angle brackets to denote an average over the ensemble. The mean, for example, is given by

$$\langle T_0(t) \rangle \equiv \lim_{N \to \infty} \frac{1}{N} \sum_{\epsilon=1}^{N} T_0(t, \epsilon) \qquad (134)$$

and the autocovariance function is given by

$$\langle \delta T_0(t) \delta T_0(t + \tau) \rangle \equiv \lim_{N \to \infty} \frac{1}{N} \sum_{\epsilon=1}^{N} \delta T_0(t, \epsilon) \delta T_0(t + \tau, \epsilon) \qquad (135)$$

where δT_0 is the deviation from the mean. Presuming that the effects of external forcing have been subtracted, these quantities will be stationary, that is, independent of t.

There are two related techniques for determining the statistical properties of a stochastic process, namely, the Fokker-Planck and the Langevin methods. The Fokker-Planck method deals directly with the probabilities of various events and characterizes the type of process through relations between these probabilities. The Langevin method begins with a deterministic equation for the mean motion, adds a stochastic forcing with assumed statistical properties, and uses the resulting stochastic equation to derive the statistical properties of the motion. We shall employ the Langevin method, since it requires only a simple extension of our models for the mean climate.

Global Climate Model With Stochastic Forcing

To the extent that the various model parameters fluctuate on time scales typical of 'weather,' that is, well separated from climatic response times, we shall assume that their collective effect is that of a random forcing. Of course, the statistics of such forcing should be determined from detailed models such as general circulation models or from meteorological data. As a first guess, however, we shall take the amplitudes of the forcing to be distributed according to a Gaussian distribution.

The stochastic version of the simple global model discussed in sections 2 and 6 has the form

$$C(dT_0/dt) + A + BT_0 = QH_0(T_0) + \delta H(t, \epsilon) \qquad (136)$$

where δH represents the random forcing, measured in relation to the mean forcing, so that $\langle \delta H \rangle = 0$. The expression (136) represents a different equation for each member of the ensemble, that is, for each ϵ. The ensemble average of all these equations gives an expression for $\langle T_0 \rangle$, and we shall assume that $\langle T_0 \rangle$ is one of the stable steady states considered in preceding sections.
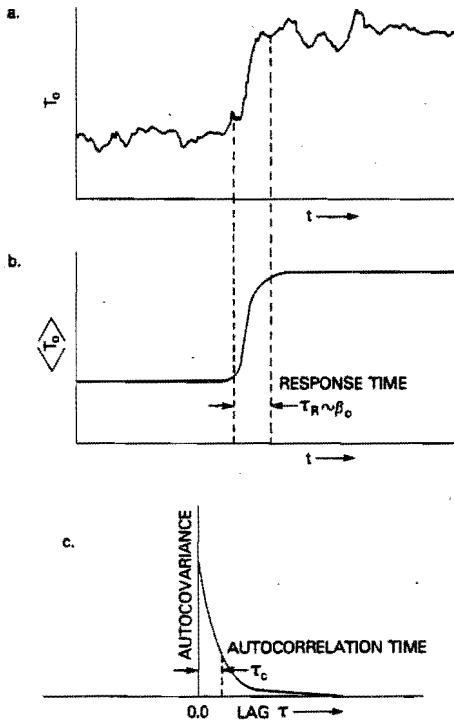
Fig. 21. Schematic illustration of the fluctuation-dissipation theorem in the weak form. (a) A typical time series of global temperature with a shift in the mean due to a step change in forcing at $t = 0$. (b) An average of many sample functions similar to the function in Figure 21a. Averaging eliminates the fluctuations, leaving only the mean, which changes from one stationary value to another during a time τ_R, the climatic response time, proportional to the sensitivity β_0. (c) Autocovariance of $\delta T_0 = T_0 - \langle T_0 \rangle$. This function decreases over a characteristic lag time τ_c, the autocorrelation time for fluctuations in T_0. If the fluctuation-dissipation theorem holds, $\tau_c = \tau_R$.

If the fluctuations in T_0 are sufficiently small, we may linearize (136) about a steady state. Upon linearizing (136) we obtain

$$C(d/dt)\delta T_0 + \lambda_0 \delta T_0 = \delta H(t, \epsilon) \tag{137}$$

where $\delta T_0 = T_0 - \langle T_0 \rangle$ and λ_0 is given by

$$\lambda_0 = QH_0/\beta_0 = B \qquad \text{with fixed albedo}$$
$$\lambda_0 = QH_0/\beta_0 = B - Q(dH_0/dT_0) \quad \text{with albedo feedback} \tag{138}$$

where $\beta_0 = Q \, dT_0/dQ$ is the sensitivity. According to section 6, λ_0 may be interpreted as the stability eigenvalue of the mean climate $\langle T_0 \rangle$. It is given by the curvature at the associated minimum of the global model potential shown in Figure 17. The formal solution to (137) is given by

$$\delta T_0(t, \epsilon) = \int_{-\infty}^{\infty} dt' \, g_0(t - t') \, \delta H(t', \epsilon) \tag{139}$$

where

$$g_0(\tau) = \frac{1}{C}\theta(\tau)e^{-\lambda_0\tau/C} \tag{140}$$

is the retarded Green's function for the linearized equation. The unit step function $\theta(\tau)$ in (140) vanishes when $\tau < 0$. As a result the response at time t depends only on the forcing at earlier times $t' < t$.

Note that the linearization requires only that δT_0 remain small. The forcing can be quite general. Thus we may apply

(139) to determine the response to deterministic changes in external heat sources as well as the response to fluctuating internal heat sources. For example, substituting a Dirac delta function for δH shows that $g_0(\tau)$ may be interpreted as the effect of a heat impulse at time t' on the temperature at time $t' + \tau$. For a constant change in heating beginning at $t' = 0$ the temperature response at time t is the integral over $g_0(\tau)$ for $\tau \leq t$. This integral grows to a final value proportional to $\lambda_0^{-1} \sim \beta_0$ after a characteristic response time given by

$$\tau_R = C/\lambda_0 = (C/QH_0)\beta_0 \tag{141}$$

So both the response time and the shift in the mean temperature are determined by the sensitivity.

The statistical properties of random variables may be determined either by specifying their 'probability distribution' or by specifying their 'moments' (see, for example, Papoulis [1965, section 5-4]). If δH assumes a Gaussian distribution, its odd moments will be zero,

$$\langle \delta H(t_1) \, \delta H(t_2) \cdots \delta H(t_{2n+1}) \rangle = 0 \tag{142}$$

and its even moments will be given by a sum of second-moment products,

$$\langle \delta H(t_1) \, \delta H(t_2) \cdots \delta H(t_{2n}) \rangle$$
$$= \sum_{\text{all pairs}} \langle \delta H(t_i) \, \delta H(t_j) \rangle \langle \delta H(t_k) \, \delta H(t_l) \rangle \cdots \tag{143}$$

As a result the statistics of δH are completely described by the second moment, or autocovariance, which we denote by Γ^H. We shall assume that the autocorrelation time of the forcing may be neglected in relation to the response time of the temperature so that we may write

$$\Gamma^H(\tau) = \langle \delta H(t) \, \delta H(t + \tau) \rangle = \gamma \delta(\tau) \tag{144}$$

where γ is a constant. This is called 'white noise' in analogy to light because the corresponding spectrum, which is given by

$$S^H(\omega) = \int_{-\infty}^{\infty} d\tau \, e^{-i\omega\tau}\Gamma^H(\tau) = \gamma \tag{145}$$

is independent of ω, the angular frequency.

Using the linear expression (139) and remembering that g_0 can be factored from any ensemble average, one can show that the moments of δT_0 also satisfy (142) and (143). Thus δT_0 is also Gaussian, and its statistics are described by its autocovariance, which we denote by Γ_{00}^T. Applying (139) gives Γ_{00}^T as a double integral over Γ^H. Using (144), we obtain

$$\Gamma_{00}^T(\tau) = \langle \delta T_0(t) \, \delta T_0(t + \tau) \rangle = (\gamma/2\lambda_0 C)e^{-\lambda_0|\tau|/C} \tag{146}$$

Note that the characteristic decay time of the autocovariance, which is the autocorrelation time τ_c, is identical to the response time for a step change in forcing,

$$\tau_c = C/\lambda_0 = \tau_R \tag{147}$$

The autocorrelation time is thus also determined by the sensitivity. The relation (147) is a special case of the more general fluctuation-dissipation relation given by

$$\Gamma_{00}^T(\tau)/\Gamma_{00}^T(0) = Cg_0(\tau) \qquad \tau > 0 \tag{148}$$

The left side of (148) is potentially measurable from climatic records. Through (139) the resulting knowledge of g_0 would allow the estimation of global temperature changes that might result from any contemplated change in global heating pro-

vided we could estimate the thermal inertia C. For a step change in heating we have seen that the response approaches the integral of g_0 over all τ and, since both sides of (148) are exponentials in τ, the integral of (148) reduces to (147). We refer to (148) as the 'strong' form of the fluctuation-dissipation relation. It determines the response at any time τ to any given forcing. We refer to the integrated version (equality of the integral of left- and right-hand sides of (148)) as the 'weak' form. It determines the response at large times to a step function in forcing. The weak form may remain a good approximation in forced dissipative systems even if the strong form does not hold at all τ [*Bell*, 1980].

Figure 21 provides an illustration of the fluctuation-dissipation relation. Shown in Figure 21*a* is a typical time series of T_0. The time series could be either measured or model generated. It contains both spontaneous fluctuations and a shift in the mean at $t = 0$. Figure 21*b* shows the mean temperature. The mean may be extracted by time averaging segments of the record shown in Figure 21*a*. If the record were model generated, the mean would be obtained by averaging an ensemble of model runs. In time τ_R the mean temperature responds to a change in mean heating. Subtracting Figure 21*b* from Figure 21*a* produces a stationary time series for $\delta T_0 = T_0 - \langle T_0 \rangle$ that has zero mean and an autocovariance with exponential form as is shown in Figure 21*c*. As is suggested by the fluctuation-dissipation relation, the autocorrelation time (indicated in the figure by τ_c) is identical to the response time τ_R.

The above results may be reexpressed in the frequency domain by Fourier transforming. Transforming (140) gives

$$g_0(\omega) = 1/(i\omega C + \lambda_0) \tag{149}$$

and transforming (146) gives the variance spectrum for the global temperature,

$$S_{00}^T(\omega) = |g_0(\omega)|^2 \gamma = \gamma/(\omega^2 C^2 + \lambda_0^2) \tag{150}$$

Again ω is the angular frequency. This spectrum is schematically illustrated in Figure 22. The figure exhibits a feature common to many climatic time series, namely, the variance increases as the frequency decreases. This concentration of variance at low frequencies is termed 'red noise.' According to the linearized feedback models, the spectrum grows as ω^{-2} and flattens below a frequency proportional to $\tau_c^{-1} = \lambda_0/C$. Note that this frequency is inversely proportional to the sensitivity.

The uncertainties in climate sensitivity discussed in section 4 imply uncertainties in the autocorrelation time of the global temperature and in the corresponding frequency dependence of the temperature spectrum. According to (138) and (147), τ_c would be equal to the radiative relaxation time C/B if albedo feedback were negligible. If this were the case, the spectrum of the global temperature would increase as ω^{-2} down to frequencies near B/C—a few tenths of a cycle per year. On the other hand, if albedo feedback is large, the stability parameter λ_0 becomes small. If the present climate is only marginally stable (such as the state labeled I in Figure 1, corresponding to the shallow minimum in Figure 17), then the autocorrelation time may be much longer than C/B, and the ω^{-2} behavior may persist to much lower frequencies. According to (150) our ability to reduce uncertainties in climate sensitivity will depend on our ability to estimate climate spectra at low frequencies.

Zonal Climate Models With Stochastic Forcing

As for the simple global mean model, fluctuation-dissipation relations can also be derived for zonal models. In zonal models we expect the response to fall off over some characteristic distance, as is illustrated for the diffusive model in Figure 20. According to the fluctuation-dissipation relation this distance approximately equals the correlation length derived from the spatial cross covariance. Regions separated by more than this characteristic distance represent independent climates. As a result we could, for example, apply the same global-type model to two such independent regions.

We shall restrict ourselves here to zonal average models with constant C. To study the zonal average models, we will follow the approach of section 6. For a basis set we shall use the eigenfunctions of the linearized energy balance equation. With this expansion the potential curvature of the global model, λ_0, will be replaced by the eigenvalues of the linearized equation, λ_n. As in section 6, the λ_n are the curvature parameters of a generalized potential. The autocorrelation times for each mode, $\tau_n = C/\lambda_n$, decrease as n increases.

Consider the class of one-dimensional stochastic models obtained by adding random forcing δH to the time-dependent version of (39):

$$C(\partial T/\partial t) + L[T] = H + \delta H \tag{151}$$

As before, we assume δH to have zero mean and to be normally distributed. We shall also take the spatial cross covariance to be given by

$$\langle \delta H(x, t) \, \delta H(y, t + \tau) \rangle = \gamma(x, y) \, \delta(\tau) \tag{152}$$

where, as before, the angle brackets indicate an ensemble average.

Linearizing (151) about a stable steady state gives

$$C(\partial/\partial t) \delta T + L[\delta T] = H'[\delta T] + \delta H \tag{153}$$

where the term H' is evaluated for the state in question.

In order to relate the fluctuations to the sensitivity, as we did for the global model, we assume that $L - H'$ has a discrete spectrum λ_n, as pictured in Figure 18, and expand δT in terms of the corresponding eigenfunctions $\psi_n(x)$ as follows:

$$\delta T(x, t) = \sum_n \delta T_n(t)\psi_n(x) \tag{154}$$

With a similar expansion for δH the individual modes will fluctuate according to

$$C(d/dt) \delta T_n + \lambda_n \delta T_n = \delta H_n \tag{155}$$

and these are coupled through

$$\langle \delta H_m(t) \, \delta H_n(t + \tau) \rangle = \gamma_{mn} \, \delta(\tau) \tag{156}$$

where

$$\gamma_{mn} = \int_0^1 dx \int_0^1 dy \, \psi_n(x) \, \psi_m(y) \, \gamma(x, y) \tag{157}$$

Since (155) is analogous to the global form (137), the autocovariance and spectrum of the δT_n are analogous to (146) and (150):

$$\Gamma_{mn}^T(\tau) = \langle \delta T_m(t) \, \delta T_n(t + \tau) \rangle$$
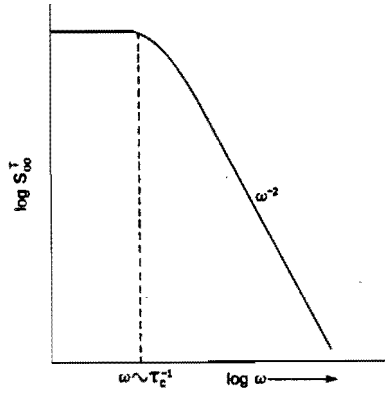
Fig. 22. Spectrum of fluctuations in T_0, given by the Fourier transform of the autocovariance function shown in Figure 21c. Most of the variance occurs below a frequency of the order of τ_c^{-1}, which, according to the fluctuation-dissipation theorem, is smallest when the sensitivity β_0 is largest.

$$= [\gamma_{mn}/(\lambda_m + \lambda_n)C][e^{-\lambda_m\tau/C}\theta(\tau) + e^{\lambda_n\tau/C}\theta(-\tau)] \qquad (158)$$

$$S_{mn}^T(\omega) = \frac{\gamma_{mn}}{(i\omega C + \lambda_m)(-i\omega C + \lambda_n)} \qquad (159)$$

Modes with successively higher values of λ_n (smaller spatial scales) have less variance, shorter autocorrelation times, and spectra which tend to be flat at frequencies such that $S_{00}^T \sim \omega^{-2}$.

As with the simple global model, (153) may be solved through the use of a retarded Green's function. The Green's function satisfies

$$[C(\partial/\partial t) + L - H']G(x, x'; t - t') = \delta(x - x')\,\delta(t - t') \qquad (160)$$

In terms of the Green's function the temperature fluctuations are given by

$$\delta T(x, t, \epsilon) = \int dx' \int dt'\, G(x, x'; t - t')\,\delta H(x', t', \epsilon) \qquad (161)$$

By using (161) and (152) to evaluate the spatial cross covariance and by performing one of the time integrals we obtain

$$\Gamma^T(x, y; \tau) = \int dx' \int dy' \int dt'\, G(x, x'; t')G(y, y'; t' + \tau)\gamma(x', y') \qquad (162)$$

This formal result is independent of the basis functions. Note that the modal expression given by (158) may be recovered from (162) by setting

$$G(x, x'; \tau) = \sum_n \psi_n(x')\,\psi_n(x')g_n(\tau)$$

where

$$g_n(\tau) = \frac{1}{C}\, e^{-\lambda_n\tau/C}\theta(\tau) \qquad (163)$$

From the orthonormality of the ψ_n it can be shown that

$$G(y, y'; t' + \tau) = C \int dz\, G(z, y'; t')\, G(z, y; \tau) \qquad (164)$$

As a result, (162) becomes

$$\Gamma^T(x, y; \tau) = C \int dz\, \Gamma^T(x, z; 0)\, G(z, y; \tau) \qquad (165)$$

If we define the inverse of the zero-lag cross covariance, $[\Gamma^T]^{-1}$, such that $\int dz [\Gamma^T]^{-1}(x, z; 0)\Gamma^T(z, y; 0) = \delta(z - y)$, then (165) gives

$$\int dz [\Gamma^T]^{-1}(x, z; 0)\Gamma^T(z, y; \tau) = CG(z, y; \tau) \qquad (166)$$

The expression (166) is a generalization of the global fluctuation-dissipation relation (148), and it is the strong form, since it applies for each τ. It gives a direct connection between the unpredictable natural variability of the steady state climate, as measured by Γ^T, and the potentially predictable response of the mean climate to an impulsive external perturbation. According to this fluctuation-dissipation relation, if the thermal inertia of the system C is known, an estimate of Γ^T from the climatic record determines G. Using G, the mean response to any perturbation (the addition of waste heat, a change in albedo, etc.) is obtained at any given latitude and time by convoluting the proposed change with G, as in (161). Consider, for example, a constant change in heating added at $x' = y$ and beginning at $t' = 0$. From (161) this change produces a response at x and at time t given by the integral over $G(x, y; \tau)$ for $0 \le \tau \le t$. For large t this integral approaches the stationary response function $G(x, y)$ discussed in section 7 and illustrated for a particular model in Figure 20. According to (166) the stationary response of the true climate to a perturbation could be estimated from the integral of $\Gamma^T(x, y; \tau)$ over all positive τ. As for the global model, low frequencies dominate, and in terms of the spatial cross spectrum we obtain

$$\int dz [\Gamma^T]^{-1}(x, z; 0)\left[\frac{1}{2}\,\mathrm{Re}\, S^T(z, y; 0) \right.$$
$$\left. + \frac{1}{\pi}\int_0^\infty \frac{d\omega}{\omega}\,\mathrm{Im}\, S^T(z, y; \omega) \right] \qquad (167)$$

In our terminology, (167) is referred to as the weak form of the zonal fluctuation-dissipation relation. It generalizes the global version (147). The zonal version relates not only the time scales of natural fluctuations and responses to perturbations but also their spatial distributions. According to (167) the spatial response may be estimated from the low-frequency cross covariance divided by the total cross covariance.

In closing this section we should recall our original assumption that the system can be divided into slow and fast components, that is, that the autocorrelation time of 'weather' is much shorter than climatic response times. Some justification for Mitchell's original stochastic treatment of sea surface temperature anomalies is provided by the relatively long radiative relaxation time of an ocean column compared to that of the atmospheric column that provides the forcing. In Budyko-Sellers models the ice-albedo feedback results in long response times, at least for the largest spatial scales, but one must also isolate the effects of the mean forcing in each mode. The stochastic treatment is less tenable for the higher modes, since, as we have seen, the response times tend to be shorter and the mean forcing less well understood.

9. DISCUSSION

It is remarkable that the zonally averaged sea level temperature for the northern hemisphere can be fitted to the simple parabolic form

$$T(x, t) \cong T_0 + T_0 \cos(2\pi t - \phi_T)P_1(x) + T_2P_2(x) \qquad (168)$$

with an rms error of only 2°C. The parameters T_0, T_1, ϕ_T, and T_2 thus give a reasonable representation of this hemispheric climate variable. An obvious goal in global climate theory is to construct models that generate these four parameters in agreement with observations and predict how the parameters change when external conditions change.

Since (168) involves only the largest space scales and the

annual time scale and since the solar heating is also describable by these same scales, we are encouraged to try simple heat balance models that connect the two. This review has surveyed and appraised recent progress toward achieving the connection.

In section 2 a sequence of mean annual models was introduced. It was shown that the mean annual global temperature T_0 can be estimated by using the most elementary radiation balance considerations provided an empirical formula for the terrestrial outgoing radiation is used. This latter includes corrections for the greenhouse effect due to the presence of infrared absorbing gases, clouds, and even the change of absolute humidity with temperature. Provided the observed present albedo is used, this estimate of T_0 is independent of transport mechanisms. The sensitivity of the climate β_0 was shown to be about twice as large for the empirical earth model as for an ideal infrared-emitting planet. The enhancement can be accounted for by the change in absolute humidity with temperature.

In order to estimate T_2, which is a measure of the mean annual pole-to-equator temperature gradient, one must introduce assumptions about how heat is redistributed on the earth's surface by the geophysical fluid system. Because diffusive terms lead naturally to the parabolic component $P_2(x)$ in the energy balance equation, it is natural to take the transport to be proportional to the gradient of temperature. For simple diffusive models the diffusion coefficient may be adjusted so that the correct amplitude T_2 is obtained. In order to estimate the sensitivity of the resulting two-mode model, more assumptions must be introduced. For example, if the earth is cooled, the ice caps expand, and the planet becomes more reflective to solar radiation. To allow for such changes, feedbacks such as cloudiness changes, changes in the transport model, and changes in the infrared formula due, for example, to lapse rate changes ought to be included. As such feedbacks remain largely unknown, they were not treated extensively in this review. Of course, they merit further attention as more empirical and theoretical information accrues.

In section 2 it was shown that the simple ice cap models are nonlinear and have solutions that exhibit a rich structure. In particular, there are at least three solutions for the present value of the solar constant. If the sun's luminosity is lowered by about 10%, the model climates experience a catastrophic transition to an ice-covered earth. This feature appears to exist even in the results produced with numerical general circulation climate models.

By introducing a heat storage term $C \, \partial T/\partial t$ to the energy balance equation and allowing the solar absorption to vary with the seasonal cycle we showed in section 3 that T_1 and ϕ_T could be estimated. It appears that reasonable values for these parameters can only be obtained if the value of the thermal inertia C is taken to be much smaller over land than over ocean. As a test of the simple seasonal model construction the four parameters T_0, T_1, ϕ_T, and T_2 were computed for the southern hemisphere by changing only the albedo and the land fraction. The test proved satisfactory enough to suggest that the main feedbacks which operate on a seasonal time scale had been included.

Section 4 concentrated upon the relationship between the quality of the parameterization formulae and their effect upon estimates of the sensitivity to solar constant changes. Each empirical formula was criticized, and the need for further work in parameterizations was emphasized.

Even with the reservations of section 4 we think that some problems of practical interest can be examined with the simple models. In section 5 we used the seasonal model with ice cap feedback to estimate the effects of changes in the earth's orbital elements. We found that the climate response to orbital changes was about an order of magnitude less than the paleoclimatic data seem to indicate. We suspect that this is a large enough discrepancy to rule out the simple instantaneously responding ice cap feedback as a prime cause of the ice ages. We emphasize that many lower-frequency feedbacks cannot be discovered by examining only the seasonal cycle. Clearly, more work can be done on this problem, and the simple models will provide a useful framework for future discussions.

Section 6 covers the stability of the simple models. In particular, it was shown that the linear stability of a solution can be deduced from the sign of the local slope of the ice line versus solar constant curve. This slope-stability theorem appears to hold for a broad class of models independent of numerical inputs. An analysis is also given for the finite amplitude time behavior of a class of models. A potential function can be constructed that yields qualitative information about the behavior of the system far from steady states. The potential function can also be thought of as a variational principle for the climate.

Section 7 presents a simple analysis of stationary perturbations to the heat balance. The analysis shows that the sensitivity for any perturbation is related to the sensitivity for solar constant changes. The relationship is shown to hold for a broad class of models.

Section 8 concludes the review with an introduction to stochastic climate models. The simple models of previous sections were linearized and allowed to have a stochastic white noise forcing. Analytical solutions are easily found for the various climate statistics. Example proofs of the fluctuation-dissipation theorem were given. Through this theorem, it was shown that information about climate sensitivity can be derived from data on natural fluctuations.

Many of the results of this review are expected to hold for more comprehensive climate models. The simple models form an intuitive base from which we can study the larger but less scrutable models. For example, when a result fails to carry over to a larger model, we immediately face the problem of discovering why. Future experiments with the large and small models may lead to valid parameterizations that can be used in the simple models. If this turns out to be true, the simple models may be able to combine the parameterization formulae found with empirical data in such a way as to play a significant role in the assessment of climate change.

APPENDIX A: CLOSED FORM GREEN'S FUNCTION

In this appendix we present a brief derivation of the Green's function for a diffusive climate model. Instead of the form (44), which converges slowly, we seek a closed form expression. We follow a notation used by *North* [1975a] in a slightly different context. Consider the differential equation

$$-\frac{D}{B} \frac{d}{dx} (1 - x^2) \frac{d}{dx} G_0(x, x') + G_0(x, x') = \delta(x - x') \quad \text{(A1)}$$

subject to the usual vanishing gradient boundary condition at the pole and equator. For $x > x'$ the equation is homogeneous and is known to have the solution [*Kamke*, 1959]

$$G_p(x, x') = A_1 P_\nu(x) + A_2 Q_\nu(x) \qquad x > x' \quad \text{(A2)}$$

where $P_\nu(x)$ and $Q_\nu(x)$ are the Legendre functions and

$$\nu = -\tfrac{1}{2} + \tfrac{1}{2}[1 - (4B/D)]^{1/2} \qquad (A3)$$

which in general may be complex. The coefficient A_2 must vanish, since $Q_\nu(x)$ diverges at the pole. Similarly, below the heat source, $x < x'$, we find [*Kamke*, 1959]

$$G_E(x, x') = A_3 f_{1\nu}(x) + A_4 f_{2\nu}(x') \qquad (A4)$$

The functions $P_\nu(x)$, $f_{1\nu}(x)$, and $f_{2\nu}(x)$ may all be related to hypergeometric functions [*Kamke*, 1959; *Erdélyi*, 1953]:

$$P_\nu(x) = F(\tfrac{1}{2} + \tfrac{1}{2}\nu, -\tfrac{1}{2}\nu, 1, 1 - x^2)$$

$$f_{1\nu}(x) = F(-\tfrac{1}{2}\nu, \tfrac{1}{2} + \tfrac{1}{2}\nu, \tfrac{1}{2}, x^2) \qquad (A5)$$

$$f_{2\nu}(x) = xF(\tfrac{1}{2} - \tfrac{1}{2}\nu, 1 + \tfrac{1}{2}\nu, \tfrac{3}{2}, x^2)$$

Power series representations may be used to evaluate any of these functions in the domain of interest. If we make use of the property

$$(d/dz)F(z, b, c, z) = (ab/c)F(a + 1, b + 1, c + 1, z) \qquad (A6)$$

and

$$F(a, b, c, 0) = 1 \qquad (A7)$$

it can be shown that A_4 must vanish to satisfy the equatorial boundary condition. Now continuity requires

$$G_p(x', x') = G_E(x', x') \qquad (A8)$$

which leads to

$$A_3 = A_1 P_\nu(x')/f_{1\nu}(x') \qquad (A9)$$

Now by integrating (A1) over an infinitesimal interval about $x = x'$ we obtain another condition,

$$-\frac{D}{B}(1 - x^2)\frac{d}{dx}G(x, x')\bigg|_{x-}^{x+} = 1 \qquad (A10)$$

which leads to the unique solution for A_1, A_3. The Green's function may now be written as

$$G_0(x, x') = fP(x)/\Omega \qquad x' \le x \le 1$$
$$\qquad\qquad\qquad\qquad\qquad\qquad (A11)$$
$$G_0(x, x') = Pf(x)/\Omega \qquad 0 \le x \le x'$$

where

$$\Omega = -(1 - x'^2)(fP' - Pf')D/B \qquad (A12)$$

where the argument x' and the indices ν, 1 have been suppressed and the prime on P and f indicates derivative.

NOTATION

Equation numbers given refer to the first use of the symbol in an equation or to equations nearest the first occurrence of the symbol in the text. In some cases a numerical value is listed which coincides with that used in the text. These values are likely to change with improved measurements and models.

A intercept in the Budyko radiation formula (7); 203.3 W m^{-2} for northern hemisphere.

$\alpha(x)$ albedo at latitude designated by x (2); cf. Table 1 for northern hemisphere.

α_p planetary albedo (2); 0.30.

a_i, a_f absorption fraction (co-albedo) of earth-atmo-

sphere system over ice and ice-free surfaces (13); 0.38; 0.70.

$\hat{a}$ average co-albedo at ice cap edge (18); 0.54.

a_0, a_2 Legendre coefficients of co-albedo (19); 0.681, -0.202.

$a(x, x_s)$ co-albedo as function of latitude and ice cap edge.

$a_1(t)$ time-dependent coefficient of $P_1(x)$ (61); cf. Table 1.

B linear coefficient in Budyko radiation formula (7); 2.09 W m^{-2} °C^{-1}.

β_0 sensitivity (5); value model-dependent, as discussed in section 4.

C effective heat capacity per unit area of earth-atmosphere system (78).

C_L, C_W C for ideal land and oceanic mixed layer; $0.16B$ years, $4.7B$ years ($B = 2.09$ W m^{-2} °C^{-1}).

D thermal diffusion coefficient (22), (33); 0.649 W m^{-2} °C^{-1} or $D/B = 0.310$.

D_2' effective D for latitude-dependent diffusion in two-mode approximation (36).

Δa change in co-albedo at the ice cap edge (99b).

e eccentricity of earth's orbit (73); 0.017 (present value).

$f_n(x)$ orthonormal eigenfunctions of the diffusion operator (47).

f_L, f_w fraction of land and water in a latitude belt for the simplified seasonal model (54).

$F(T_0)$, $F(I_0, I_2, \cdots)$ potential function for the zero- and one-dimensional models (86), (115).

$F[T]$ Lyapunov functional for the temperature field (107).

ϕ_n infinitesimal departure from a local extremum in $F(I_0, I_2, \cdots)$ (115).

g global average value of the stationary heat perturbation (121).

$g_0(\tau), g_n(\tau)$ temperature impulse-response functions for the global average or higher modes (139), (163).

$G_0(x, x')$ Green's function for the linear transport operator in the energy balance equation (42).

$G(x, z)$ Green's function for the transport combined with linearized ice-albedo feedback (131).

G_{ijk} mode-coupling coefficients (64).

$G(x, x_0; t - t')$ Green's function for the linearized time-dependent energy balance equation (160).

γ Budyko transport coefficient (34); also the strength of global white noise forcing in (144).

$\gamma(x, y)$ spatial cross covariance of the white noise forcing in (152).

γ_{mn} expansion coefficients of $\gamma(x, y)$ in the ψ_n basis (157).

$\Gamma^H(\tau)$ autocovariance of global white noise forcing at lag time τ (144).

$\Gamma_{00}^T(\tau)$ autocovariance of global temperature fluctuations at lag time τ (146).

$\Gamma^T(x, y; \tau)$ spatial cross covariance of zonal temperature fluctuations at lag time τ (162).

$\Gamma_{mn}^T(\tau)$ expansion coefficients of $\Gamma^T(x, y; \tau)$ in the ψ_n basis (158).

$H_n(x_s)$ Legendre polynomial amplitude of solar heat absorbed (29).

$h_n(x_s)$ amplitude of solar heat absorbed with respect to the eigenfunctions $f_n(x)$ (91b).

$I, I(x), I(x, t)$ infrared radiation to space (7), also Table 1, watts per square meter.

I_s I evaluated at $x = x_s$ (90).

I_n Legendre or $f_n(x)$ amplitude for I (90).

$L[T]$ a linear operator (40).

L_n, l_n eigenvalues of the linear operator in an energy balance equation (29), (49).

λ stability eigenvalue (98).

ν an empirical transfer coefficient coupling land and water areas in the seasonal model (56).

$\psi_n(x)$ orthonormal eigenfunctions of the linearized steady state energy balance equation, with eigenvalues given by the stability parameter λ; in the absence of ice-albedo feedback, $\psi_n = f_n$ and $\lambda_n = l_n$ (154).

$P_n(x)$ Legendre polynomial.

Q, Q_0 solar constant divided by 4 (8) (subscript zero denotes present value (335 W m^{-2} in section 2, 340 W m^{-2} in section 3)).

R radius of earth (1).

σ Stefan-Boltzmann constant (1), equal to 0.5669×10^{-7} W m^{-2} K^{-4}.

σ_0 solar constant, see Q, Q_0 (1).

$S(x), S(x, t)$ theoretical distribution of solar heat energy reaching top of the atmosphere (2), (3), Table 1, (74).

$S_n(t)$ Legendre mode amplitude for $S(x, t)$ (3), (61), Table 1, (74).

S^H spectrum of random forcing (145).

$S_{\infty}^{T}(\omega)$ spectrum of global temperature fluctuations (150).

$S^T(x, y, \omega)$ spatial cross spectrum of zonal temperature fluctuations (167).

$S_{mn}^{T}(\omega)$ cross spectrum of temperature fluctuations in modes of m and n (159).

$T, T(x)$ zonally averaged 1000-mbar level temperature field (when t does not appear, annual averaging is implied) Table 1.

T_R planetary radiative temperature (1).

T_n Legendre mode amplitude for $T(x)$ or $T(x, t)$; T_0 is the planetary average temperature.

T_s temperature at ice cap edge (16); Budyko's rule: $T_s = -10°C$.

τ, τ_c, τ_R lag time, climatic autocorrelation time, climatic response time (values depend on β_0).

$u(x)$ normalized distribution of added heat flux (121).

x sine of latitude (2).

x_s sine of latitude at ice cap edge (13); for the present climate, $x_s = 0.95$.

References

Adem, J., On the theory of the general circulation of the atmosphere, *Tellus, 14*, 102–115, 1962.

Ångström, A., Energiezufuhr und Temperatur auf verschiedenen Breitgraden, *Beitr. Geophyz., 15*, 1–13, 1928.

Bell, T. L., Climate sensitivity from fluctuation dissipation: Some simple model tests, *J. Atmos. Sci., 37*, 1700–1707, 1980.

Berger, A. L., Long-term variations of caloric insolation resulting from the earth's orbital elements, *Quat. Res. N. Y., 9*, 139–167, 1978.

Budyko, M. I., On the origin of glacial epochs, *Meteorol. Gidrol., 2*, 3–8, 1968.

Budyko, M. I., The effect of solar radiation variations on the climate of the earth, *Tellus, 21*, 611–619, 1969.

Budyko, M. I., The future climate, *Eos Trans. AGU, 53*, 868–870, 1972.

Budyko, M. I., On present-day climatic changes, *Tellus, 29*, 193–204, 1977.

Cahalan, R. F., and G. R. North, A stability theorem for energy-balance climate models, *J. Atmos. Sci., 36*, 1205–1216, 1979.

Cess, R. D., Climate change: An appraisal of atmospheric feedback mechanisms employing zonal climatology, *J. Atmos. Sci., 33*, 1831–1843, 1976.

Cess, R. D., Biosphere-albedo feedback and climate modeling, *J. Atmos. Sci., 35*, 1765–1768, 1978.

Cess, R. D., and V. Ramanathan, Averaging of infrared cloud opacities for climate modeling, *J. Atmos. Sci., 35*, 675–679, 1978.

Cess, R. D., and J. C. Wronka, Ice ages and the Milankovitch theory: A study of interactive climate feedback mechanisms, *Tellus, 31*, 185–192, 1979.

Chýlek, P., and J. A. Coakley, Analytical analysis of a Budyko-type climate model, *J. Atmos. Sci., 32*, 675–679, 1974.

Climap Project Members, The surface of the ice-age earth, *Science, 191*, 1131–1137, 1976.

Coakley, J. A., Feedbacks in vertical-column energy balance models, *J. Atmos. Sci., 34*, 465–470, 1977.

Coakley, J. A., A study of climate sensitivity using a simple energy balance climate model, *J. Atmos. Sci., 36*, 260–269, 1979.

Coakley, J. A., and B. Wielicki, Testing energy balance climate models, *J. Atmos. Sci., 36*, 2031–2039, 1979.

Courant, R., and D. Hilbert, *Methods of Mathematical Physics*, vol. 1, 560 pp., Interscience, New York, 1953.

Crafoord, C., and E. Källén, A note on the condition for existence of more than one steady state solution in Budyko-Sellers type models, *J. Atmos. Sci., 35*, 1123–1125, 1978.

Drazin, P. G., and D. H. Griffel, On the branching structure of diffusive climatological models, *J. Atmos. Sci., 34*, 1858–1867, 1977.

Ellis, J. S., T. H. Vonder Haar, S. Levitus, and A. H. Oort, The annual variation in the global heat balance of the earth, *J. Geophys. Res., 83*, 1959–1962, 1978.

Erdélyi, E. (Ed.), *Higher Transcendental Functions*, vol. 1, 302 pp., McGraw-Hill, New York, 1953.

Eriksson, E., Air-ocean-ice cap interactions in relation to climatic fluctuations and glaciation cycles, *Meteorol. Monogr., 8*, 68–92, 1968.

Fraedrich, K., Structural and stochastic analysis of a zero-dimensional climate system, *Q. J. R. Meteorol. Soc., 104*, 461–474, 1978.

Frankignoul, C., and K. Hasselmann, Stochastic climate models, II, Application to sea-surface temperature anomalies and thermocline variability, *Tellus, 29*, 289–305, 1977.

Frankignoul, C., and P. Müller, Quasi-geostrophic response of an infinite β-plane ocean to stochastic forcing by the atmosphere, *J. Phys. Oceanogr., 9*, 104–127, 1979.

Frederiksen, J. S., Nonlinear albedo-temperature coupling in climate models, *J. Atmos. Sci., 33*, 2267–2272, 1976.

Fritz, S., The heating distribution in the atmosphere and climatic change, in *Dynamics of Climate*, 136 pp., Pergamon, New York, 1960.

Gal-Chen, T., and S. H. Schneider, Energy balance climate modeling: Comparison of radiative and dynamic feedback mechanisms, *Tellus, 28*, 108–121, 1976.

Gates, W. L., and M. E. Schlesinger, Numerical simulation of the January and July global climate with a two-level atmospheric model, *J. Atmos. Sci., 34*, 36–76, 1977.

Ghil, M., Climate stability for a Sellers-type model, *J. Atmos. Sci., 33*, 3–20, 1976.

Ghil, M., Internal climatic mechanisms participating in glaciation cycles, in *Climate Variations and Variability: Facts and Theories*, D. Reidel, Hingham, Mass., in press, 1981.

Golitsyn, G., and I. Mokhov, Stability and extremal properties of climate models, *Izv. Acad. Sci. USSR Atmos. Oceanic Phys.*, Engl. Transl., *14*, 271–277, 1978.

Hansen, J. E., W. C. Wang, and A. A. Lacis, Mount Agung eruption provides test of a global climatic perturbation, *Science, 199*, 1065–1068, 1978.

Hart, M. H., The evolution of the atmosphere of the earth, *Icarus, 33*, 23–39, 1978.

Hartmann, D. L., and D. A. Short, On the role of zonal asymmetries in climate change, *J. Atmos. Sci., 36*, 519–528, 1979.

Hartmann, D. L., and D. A. Short, On the use of earth radiation budget statistics for studies of clouds and climate, *J. Atmos. Sci., 37*, 1233–1250, 1980.

Hasselmann, K., Stochastic climate models, I, Theory, *Tellus, 28*, 473–484, 1976.

Hays, J. D., J. Imbrie, and N. J. Shackleton, Variations in the earth's orbit: Pacemaker of the ice ages, *Science, 194*, 1121–1132, 1976.

Held, I. M., The tropospheric lapse rate and climatic sensitivity: Experiments with a two-level atmospheric model, *J. Atmos. Sci., 35*, 2083–2098, 1978.

Held, I. M., and M. Suarez, Simple albedo feedback models of the icecaps, *Tellus, 36*, 613–629, 1974.

Held, I. M., and M. Suarez, A two-level primitive equation atmospheric model designed for climatic sensitivity experiments, *J. Atmos. Sci., 35*, 206–229, 1978.

Hickey, J. R., et al., Initial solar irradiance determinations from Nimbus 7 cavity radiometer measurements, *Science, 208*, 281–283, 1980.

Jenkins, G. M., and D. G. Watts, *Spectral Analysis and Its Applications*, 525 pp., Holden-Day, San Francisco, Calif., 1968.

Källén, E., C. Crafoord, and M. Ghil, Free oscillations in a climate model with ice sheet dynamics, *J. Atmos. Sci., 36*, 2292–2303, 1979.

Kamke, E., *Differentialgleichungen, Lösungenmethoden und Lösungen*, vol. 1, 3rd ed., 666 pp., Chelsea, New York, 1959.

Kells, L. C., Stochastic analogies to diffusive climate models, 1976 GFD Summer Program Lecture Notes, pp. 121–126, Woods Hole Oceanogr. Inst., Woods Hole, Mass., 1976.

Leith, C. E., Climate response and fluctuation-dissipation, *J. Atmos. Sci., 32*, 2022–2026, 1975.

Leith, C. E., Predictability of climate, *Nature, 276*, 352–356, 1978.

Lemke, P., Stochastic climate models, III, Application to zonally averaged energy models, *Tellus, 29*, 385–392, 1977.

Lian, M. S., and R. D. Cess, Energy balance climate models: A reappraisal of ice-albedo feedback, *J. Atmos. Sci., 34*, 1058–1062, 1977.

Lin, C. A., The effect of nonlinear diffusive transport in a simple climate model, *J. Atmos. Sci., 35*, 337–340, 1978.

Lindzen, R. S., and B. Farrell, Some realistic modifications of simple climate models, *J. Atmos. Sci., 34*, 1487–1501, 1977.

Lorenz, E. N., Forced and free variations of weather and climate, *J. Atmos. Sci., 36*, 1367–1376, 1979.

Manabe, S., and R. T. Wetherald, Thermal equilibrium of the atmosphere with a given distribution of relative humidity, *J. Atmos. Sci., 24*, 241–259, 1967.

Manabe, S., and R. T. Wetherald, The effects of doubling the CO_2 concentration on the climate of a general circulation model, *J. Atmos. Sci., 32*, 3–15, 1975.

Manabe, S., K. Bryan, and M. J. Spelman, A global ocean-atmosphere climate model with seasonal variation for future studies of climate sensitivity, *Dyn. Atmos. Oceans, 3*, 393–426, 1979.

Mass, C., and S. H. Schneider, Statistical evidence on the influence of sunspots and volcanic dust on long-term temperature records, *J. Atmos. Sci., 34*, 1995–2004, 1977.

Milankovitch, M., Canon of insolation and the ice age problem (in Yugoslavian), *K. Serb. Acad. Beogr. Spec. Publ., 132*, 1941. (English translation, 482 pp., Israel Program for Scientific Translations, Jerusalem, 1969.)

Mitchell, J. M., Jr., Stochastic models of air-sea interaction and climatic fluctuation, Symposium on the Arctic Heat Budget and Atmospheric Circulation, Lake Arrowhead, California, 1966, *Mem. RN-5233-NSF*, Rand Corp., Santa Monica, Calif., 1966.

Newman, M. J., and R. T. Rood, Implication of solar evolution for the earth's early atmosphere, *Science, 198*, 1035–1037, 1977.

North, G. R., Analytical solution to a simple climate model with diffusive heat transport, *J. Atmos. Sci., 32*, 1301–1307, 1975a.

North, G. R., Theory of energy-balance climate models, *J. Atmos. Sci., 32*, 2033–2043, 1975b.

North, G. R., Analytical theories of climate, 1976 GFD Summer Program Lecture Notes, pp. 46–56, Woods Hole Oceanogr. Inst., Woods Hole, Mass., 1976.

North, G. R., and J. A. Coakley, Simple seasonal climate models, *Meteorol. Gidrol., 5*, 26–32, 1978.

North, G. R., and J. A. Coakley, Differences between seasonal and mean annual energy balance model calculations of climate and climate sensitivity, *J. Atmos. Sci., 36*, 1189–1204, 1979.

North, G. R., P. B. James, and R. F. Cahalan, Simple climate models with latitude-dependent diffusive heat transport, paper presented at Fall Meeting, AGU, San Francisco, Calif., Dec. 1977.

North, G. R., L. Howard, D. Pollard, and B. Wielicki, Variational formulation of Budyko-Sellers climate models, *J. Atmos. Sci., 36*, 255–259, 1979.

Oerlemans, J., and H. M. Van den Dool, Energy balance climate models: Stability experiments with a refined albedo and updated coefficients for infrared radiation, *J. Atmos. Sci., 35*, 371–381, 1978.

Ohring, G., and P. Clapp, The effect of changes in cloud amount on the net radiation at the top of the atmosphere, *J. Atmos. Sci., 37*, 447–454, 1980.

Öpik, E. J., Climatic changes in cosmic perspective, *Icarus, 4*, 289–307, 1965.

Owen, T., R. D. Cess, and V. Ramanathan, Enhanced CO_2 greenhouse to compensate for reduced solar luminosity on early earth, *Nature, 277*, 640–642, 1979.

Paltridge, G. W., Global dynamics and climate change—A system of minimum entropy exchange, *Q. J. R. Meteorol. Soc., 101*, 475–484, 1975.

Paltridge, G. W., The steady-state format of global climate, *Q. J. R. Meteorol. Soc., 104*, 927–945, 1978.

Papoulis, A., *Probability, Random Variables and Stochastic Processes*, 583 pp., McGraw-Hill, 1965.

Pollard, D., An investigation of the astronomical theory of the ice ages using a simple climate-ice sheet model, *Nature, 272*, 233–235, 1978.

Prigogine, I., *Introduction to Thermodynamics of Irreversible Processes*, 3rd ed., 147 pp., Wiley-Interscience, New York, 1968.

Ramanathan, V., Interactions between ice-albedo, lapse-rate, and cloud-top feedbacks: An analysis of the nonlinear response of a GCM climate model, *J. Atmos. Sci., 34*, 1885–1897, 1977.

Ramanathan, V., and J. A. Coakley, Climate modeling through radiative convective models, *Rev. Geophys. Space Phys., 16*, 465–489, 1978.

Ramanathan, V., M. S. Lian, and R. D. Cess, Increased atmospheric CO_2 zonal and seasonal estimates of the effect on the radiative energy balance and surface temperature, *J. Geophys. Res., 84*, 4949–4958, 1979.

Robock, A., Internally and externally caused climate change, *J. Atmos. Sci., 35*, 1111–1122, 1978.

Sagan, C., and G. Mullen, Earth and Mars: Evolution of atmospheres and surface temperatures, *Science, 177*, 52–56, 1972.

Salmún, H., Stationary perturbation theory for simple climate models, M.S. thesis, 55 pp., Dep. of Phys., Univ. of Mo., St. Louis, 1979.

Salmún, H., R. F. Cahalan, and G. R. North, Latitude-dependent sensitivity to stationary perturbations in simple climate models, *J. Atmos. Sci., 37*, 1874–1879, 1980.

Saltzman, B., A survey of statistical-dynamical models of the terrestrial climate, *Adv. Geophys., 20*, 183–303, 1978.

Saltzman, B., and A. Vernekar, Note on the effect of earth orbital radiation variations on climate, *J. Geophys. Res., 76*, 4195–4197, 1971.

Schneider, S. H., and R. Dickinson, Climate modeling, *Rev. Geophys. Space Phys., 12*, 447–493, 1974.

Schneider, S. H., and T. Gal-Chen, Numerical experiments in climate stability, *J. Geophys. Res., 78*, 6182–6194, 1973.

Schneider, E. K., and R. Lindzen, Axially symmetric steady-state models of the basic state for instability and climate studies, I, Linear calculations, *J. Atmos. Sci., 34*, 263–279, 1977.

Schneider, S. H., and C. Mass, Volcanic dust, sunspots, and temperature trends, *Science, 190*, 741–746, 1975.

Sellers, W. D., *Physical Climatology*, 272 pp., University of Chicago Press, Chicago, Ill., 1965.

Sellers, W. D., A climate model based on the energy balance of the earth-atmosphere system, *J. Appl. Meteorol., 8*, 392–400, 1969.

Sellers, W. D., Note on the effect of changes in the earth's obliquity

on the distribution of mean annual sea-level temperature, *J. Appl. Meteorol.*, *9*, 960–961, 1970.

Sellers, W. D., A new global climatic model, *J. Appl. Meteorol.*, *12*, 241–254, 1973.

Sellers, W. D., Climate models and variation in the solar constant, *Geofis. Int.*, *14*, 303–315, 1974.

Stone, P. H., The effect of large-scale eddies on climatic change, *J. Atmos. Sci.*, *30*, 521–529, 1973.

Stone, P. H., Constraints on dynamical transports of energy on a spherical planet, *Dyn. Oceans Atmos.*, *2*, 123–139, 1978.

Su, C. H., and D. Y. Hsieh, Stability of the Budyko climate model, *J. Atmos. Sci.*, *33*, 2273–2275, 1976.

Suarez, M. J., and I. M. Held, Note on modeling climate response to orbital parameter variations, *Nature*, *263*, 46–47, 1976.

Suarez, M. J., and I. M. Held, The sensitivity of an energy-balance climate model to variations in the orbital parameters, *J. Geophys. Res.*, *84*, 4825–4836, 1979.

Thompson, S. L., and S. H. Schneider, A seasonal zonal energy balance climate model with an interactive lower layer, *J. Geophys. Res.*, *84*, 2401–2414, 1979.

Vernekar, A. D., Long-term global variations of incoming solar radiation, *Meteorol. Monogr.*, *34*, 21 pp., 1971.

Warren, S., and S. H. Schneider, Seasonal simulation as a test for uncertainties in the parameterizations of a Budyko-Sellers zonal climate model, *J. Atmos. Sci.*, *36*, 1377–1391, 1979.

Weertman, J., Milankovitch solar radiation variations and ice age ice sheet sizes, *Nature*, *261*, 17–20, 1976.

Wetherald, R. T., and S. Manabe, Response of the joint ocean-atmosphere model to the seasonal variation of the solar radiation, *Mon. Weather Rev.*, *100*, 42–58, 1972.

Wetherald, R. T., and S. Manabe, The effects of changing the solar constant on the climate of a general circulation model, *J. Atmos. Sci.*, *32*, 2044–2059, 1975.

Willson, R. C., C. H. Duncan, and J. Geist, Direct measurement of solar luminosity variation, *Science*, *207*, 177–179, 1980.